MISCELLANEOUS PAPER H-78-5

AN OPEN-COAST MATHEMATICAL STORM SURGE MODEL WITH COASTAL FLOODING FOR LOUISIANA

Report 1

THEORY AND APPLICATION

by

John J. Wanstrath

Hydraulics Laboratory
U. S. Army Engineer Waterways Experiment Station
P. O. Box 631, Vicksburg, Miss. 39180

February 1978
Report 1 of a Series

Approved For Public Release; Distribution Unlimited
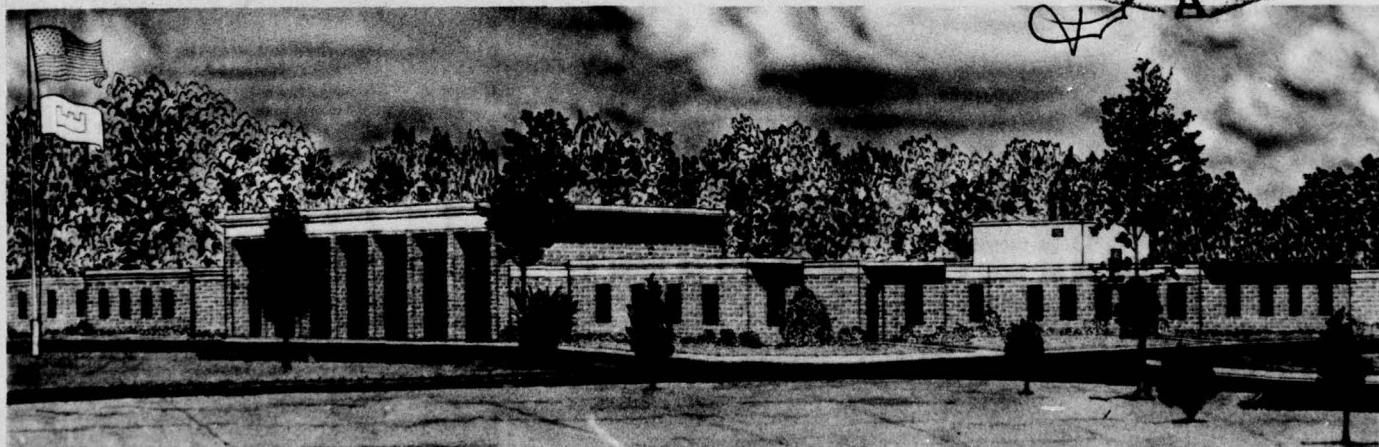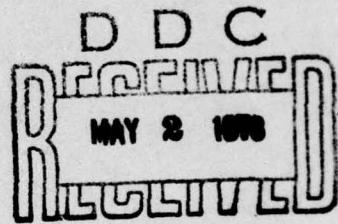
Prepared for U. S. Army Engineer District, New Orleans
New Orleans, Louisiana 70160

DISCLAIMER NOTICE

THIS DOCUMENT IS BEST QUALITY PRACTICABLE. THE COPY FURNISHED TO DDC CONTAINED A SIGNIFICANT NUMBER OF PAGES WHICH DO NOT REPRODUCE LEGIBLY.

REPORT DOCUMENTATION PAGE	READ INSTRUCTIONS BEFORE COMPLETING FORM

1. REPORT NUMBER	2. GOVT ACCESSION NO.	3. RECIPIENT'S CATALOG NUMBER
Miscellaneous Paper H-78-5 WES-MP-H-78-5-1		

4. TITLE (and Subtitle)	5. TYPE OF REPORT & PERIOD COVERED
AN OPEN-COAST MATHEMATICAL STORM SURGE MODEL WITH COASTAL FLOODING FOR LOUISIANA; Report 1, THEORY AND APPLICATION	Report 1 of a series
	6. PERFORMING ORG. REPORT NUMBER
	Miscellaneous paper

7. AUTHOR(s)	8. CONTRACT OR GRANT NUMBER(s)
John J. Wanstrath	

9. PERFORMING ORGANIZATION NAME AND ADDRESS	10. PROGRAM ELEMENT, PROJECT, TASK AREA & WORK UNIT NUMBERS
U. S. Army Engineer Waterways Experiment Station Hydraulic Laboratory P. O. Box 631, Vicksburg, Miss. 39180	

11. CONTROLLING OFFICE NAME AND ADDRESS	12. REPORT DATE
U. S. Army Engineer District, New Orleans P. O. Box 60267 New Orleans, La. 70160	Feb 78
	13. NUMBER OF PAGES
	102 101 p.

14. MONITORING AGENCY NAME & ADDRESS(if different from Controlling Office)	15. SECURITY CLASS. (of this report)
	Unclassified
	15a. DECLASSIFICATION/DOWNGRADING SCHEDULE

16. DISTRIBUTION STATEMENT (of this Report)

Approved for public release; distribution unlimited.

17. DISTRIBUTION STATEMENT (of the abstract entered in Block 20, if different from Report)

18. SUPPLEMENTARY NOTES

19. KEY WORDS (Continue on reverse side if necessary and identify by block number)

Computer programs	Mathematical models
Conformal mapping	Storm surges
Hydrodynamics	Water waves
Long waves	

20. ABSTRACT (Continue on reverse side if necessary and identify by block number)

A two-dimensional time-dependent, open-coast, long-wave, shallow-water model is presented. The model employs an orthogonal curvilinear coordinate system with telescoping computing cells. This permits greater resolution of the wave in the nearshore coastal region where principal interest is focused rather than at the continental shelf break or at far lateral distances from the region. The model treats the coastline as a finite height barrier which

(Continued)

DD FORM 1473 EDITION OF 1 NOV 65 IS OBSOLETE
1 JAN 73

038100

20. ABSTRACT (Continued)

is broken with bay entrances. Coastal overtopping and bay communication with the open sea provide the means for the transport of water across the nominal coastline. Mass is conserved with all water lost from the ocean during the flood stage being stored in discrete bay ponding areas. Each ponding area is described by its particular storage area curve and its particular series of coastline computing grid segments. A prediction/correction method is employed for the computation of the coastal water level.

The model has been employed in various tide and storm surge studies. In particular, surge results are presented from four historical hurricanes that affected the Louisiana coast.

The numerical programs are documented in Report 2 of this series.

PREFACE

The investigation reported herein was conducted in response to a request from the U. S. Army Engineer District, New Orleans (NOD). Funds were authorized by NOD on 3 January 1977.

The study was conducted by Dr. John J. Wanstrath of the Coastal Branch, Wave Dynamics Division, Hydraulics Laboratory, U. S. Army Engineer Waterways Experiment Station (WES), under the general supervision of Dr. C. L. Vincent, Chief of the Coastal Branch, Dr. R. W. Whalin, Chief of the Wave Dynamics Division, and Mr. H. B. Simmons, Chief of the Hydraulics Laboratory.

Director of WES during the conduct of the investigation and the preparation and publication of this report was COL John L. Cannon, CE. Technical Director was Mr. F. R. Brown.

1

CONTENTS

CONVERSION FACTORS, METRIC (SI) TO U. S. CUSTOMARY AND
U. S. CUSTOMARY TO METRIC (SI) UNITS OF MEASUREMENT

Units of measurement used in this report can be converted as follows:

Multiply	By	To Obtain
Metric (SI) to U. S. Customary		
metres	3.280839	feet
kilometres	0.5399568	miles (U. S. nautical)
metres per second	3.280839	feet per second
square centimetres per second	0.1550	square inches per second
millibars	0.01450377	pounds per square inch
U. S. Customary to Metric (SI)		
inches	25.4	millimetres
feet	0.3048	metres
miles (U. S. nautical)	1.852	kilometres
miles (U. S. statute)	1.609344	kilometres
square feet	0.09290304	square metres
cubic feet	0.02831685	cubic metres
pounds (force) per square inch	6894.757	pascals
feet per second	0.3048	metres per second
miles per hour (U. S. statute)	1.609344	kilometres per hour
degrees (angle)	0.01745329	radians

AN OPEN-COAST MATHEMATICAL STORM SURGE MODEL WITH

COASTAL FLOODING FOR LOUISIANA

THEORY AND APPLICATION

PART I: INTRODUCTION

1. Three-dimensional partial differential equations govern the motion of an infinitesimal fluid element. These equations result from basic considerations of mass conservation and Newton's second law of motion. The assumptions involving the incompressibility and homogeneity of the water, negligible vertical accelerations of the fluid parcel, reasonably uniform horizontal flow over the fluid depth, and others result in the classical, vertically integrated long-wave equations of motion and mass conservation. Energy is supplied at the free surface, in general, through the action of the wind and dissipated at the seabed through friction. The system of equations is time-dependent, two-dimensional in terms of the horizontal coordinates, and readily integrable through numerical techniques. These equations are applicable to the study of storm surge generation[1] on the continental shelf and to the degree that the assumptions are valid, nearshore astronomical tide simulation.

2. In the past, numerical integration of the two-dimensional as well as the three-dimensional equations of motion have been performed using rectilinear grids. Recently, curvilinear coordinates[2,3,4] have been employed in two-dimensional models, with particular applications to free and forced long-wave simulations for large (hundreds of miles*) open-coast stretches of the continental shelf.

3. Open-coast curvilinear models are considered superior to rectilinear models because rectilinear models must represent the coast boundary as a series of straight-line segments connected at right angles.

---

* A table of factors for converting metric (SI) units of measurement to U. S. customary units and U. S. customary units to metric (SI) units is presented on page 3.

Spurious oscillations are injected into the calculation by the boundary. Furthermore, the stair-step boundary must retain more water over that natural coastal configuration where water is free to move artificially unobstructed and in accord with the forces.

4. The use of any of the previously mentioned open-coast models in simulating circulation and water level conditions is made difficult because of the requirement of specifying appropriate boundary conditions. This is especially the case in the nearshore region where these models simulate the coast boundary as an infinitely high, continuous wall. This boundary condition neglects overtopping of low-lying land and bay communication with the open sea. These coastal processes have a considerable effect on the nearshore water levels and fluid velocities. Furthermore, it is precisely this zone where much environmental interest is focused and the use of numerical models should prove beneficial.

5. This report describes a more appropriate open-coast boundary condition and presents results from four historical hurricane surges which affected the Louisiana coast from Atchafalaya Bay to the Mississippi River. The boundary conditions is termed the Finite Height Barrier Coast (FHBC) and is incorporated into a two-dimensional model that employs an orthogonal curvilinear coordinate system with telescoping computing cells. This hydrodynamic model with the FHBC is named SSURGE III. In a companion report,[5] results from other verification studies of SSURGE III are presented.

6. Three numerical programs are required for staging the production of surge or tide computations. The first numerical program determines the conformal mapping coefficients for the particular study region of the continental shelf. The actual coastline, as seen on National Ocean Survey (NOS) nautical charts, is smoothed relative to portraying small-scale features. This continuous coastline and a deep-sea boundary curve (perhaps, following the 300- or 600-ft isobath) are the input to the conformal mapping program. The coefficients are determined and input to the second numerical program which determines the computing grid data relative to a particular design by the user. The grid data are, in part, the input to the SSURGE III program. Other

5

input includes the shelf bathymetry, FHBC data, hydrograph and velocity output locations, and other readily determinable parameters. In actual practice, the entire process is not time-consuming or expensive.

PART II: CONFORMAL MAPPING

7. It is desired to conformally map a spatial region of prototype space of the continental shelf into a rectangle in a mathematical image plane in which the coastline and deep-sea boundary curves are specifically transformed into the image plane as constant values of η .* Figure 1 shows the details of the transformation.

8. It can be shown[3] that a conformal transformation satisfying the above constraints is

$$x(\xi,\eta) = \xi + \sum_{n=1}^{N} (B_n \sinh nk\eta + C_n \cosh nk\eta) \sin nk\xi \qquad (1)$$

and

$$y(\xi,\eta) = B_o + \eta + \sum_{n=1}^{N} (B_n \cosh nk\eta + C_n \sinh nk\eta) \cos nk\xi \qquad (2)$$

where

$$k = \pi/\lambda$$
$$0 \le x \le \lambda \; ; \; 0 \le \xi \le \lambda \qquad (3)$$
$$-\beta \le \eta \le \beta$$

The N values of B_n and C_n and B_o constitute the bi-curve fitting conformal mapping coefficients. These coefficients are determined by matching the prototype coastline and sea boundary curves at $\eta = \pm \beta$, respectively, β also being a parameter to be determined. An iterative procedure is required for determining β and the coefficients.[3] Essentially, the procedure is terminated after convergence of β and the coefficients or after the transform-generated coastline and sea boundary curves are in good portrayal of those specified (personal view of the user). Typical standard deviation between transform-generated and prototype (slightly smoothed version) over the length of the curve is of the order of 2000 ft. This is achieved with 40 iterations,

---

* For convenience, symbols and unusual abbreviations are listed and defined in the Notation (Appendix A).

7
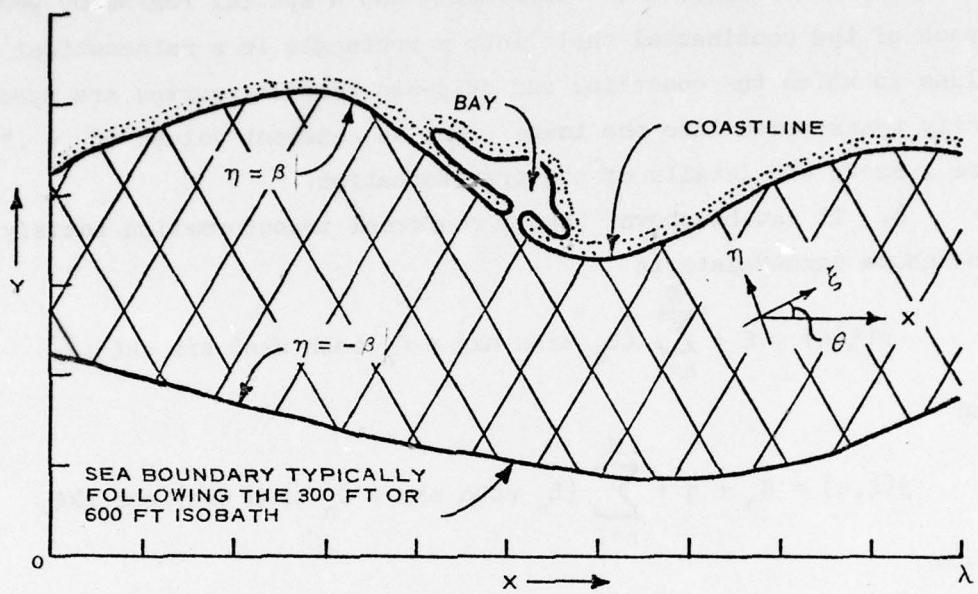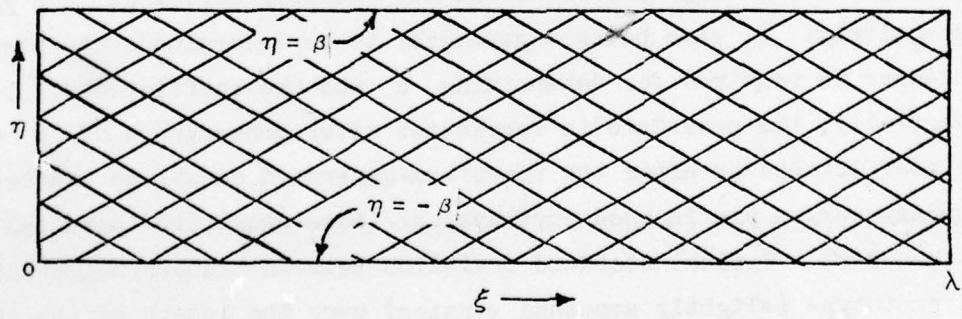
a. PROTOTYPE SPACE

b. IMAGE SPACE

Figure 1.   Conformal transformation mapping prototype space into
image space

8

N = 100 and at a cost of 9 min of CDC 6600 central processing time. Furthermore, the conformal mapping procedure need only be accomplished once for any large stretch of continental shelf. The computing grids appropriate to areas within that region are generated depending on the nature of the particular study, using the mapping coefficients previously determined. The computer cost in generating the grid is inconsequential to the personnel time required in the grid makeup or assigning the cell-averaged fluid depth. The cost in generating a grid covering a relatively small extent of coast must be weighed against a large grid of similar high resolution over a long reach of coastline which costs more per prototype hour and even more so when numerous simulations are required.

Stretched Shelf Coordinate System

9. Consider the transform-generated coastline and sea boundary curves shown in Figure 2. The orthogonal curvilinear mesh associated with the (ξ, η) coordinates in prototype space is designated the shelf coordinate system. The display of that system in prototype space is shown in Figure 2a and its image in Figure 2b. Notice that only a portion of the entire shelf mapped area is subsequently employed for long-wave computations. Furthermore, the calculations cannot readily be performed in the image space because the cells are unevenly spaced. Centered computations are a prerequisite for finite differencing of partial differential equations. To provide an evenly spaced computing grid and, at the same time, to obtain the desired spatial resolution with the fewest possible computational points require a second transformation. This transformation preserves the orthogonal property and allows for the independent stretching of ξ and of η. The grid resulting from the second transformation is the evenly spaced computing grid, Figure 2c. The coordinate system is termed the stretched shelf coordinate system (S, T).

10. The stretched shelf coordinate system is generated by independently transforming the ξ and η axes in the following manner:

a. Given the nearshore region of principal interest, the values of ξ along the coastline are determined which will produce a constant relatively fine increment of coastline arc length, S_p. In this area of prime interest, the line BC in Figure 2a, the constant increment of arc length is equal to ΔS. However, regions AB and CD show that for the same ΔS as above, there is a relative expansion of the increment of the coastline arc length. The functional relation between ξ and S is

$$S = S(S_p(\xi)) \tag{4}$$

where the expansion of S_p with respect to S is specified by an (arbitrary) expression of the form

a. PROTOTYPE SPACE (X, Y)

b. IMAGE SPACE (ξ, η)

c. COMPUTING SPACE (S, T)
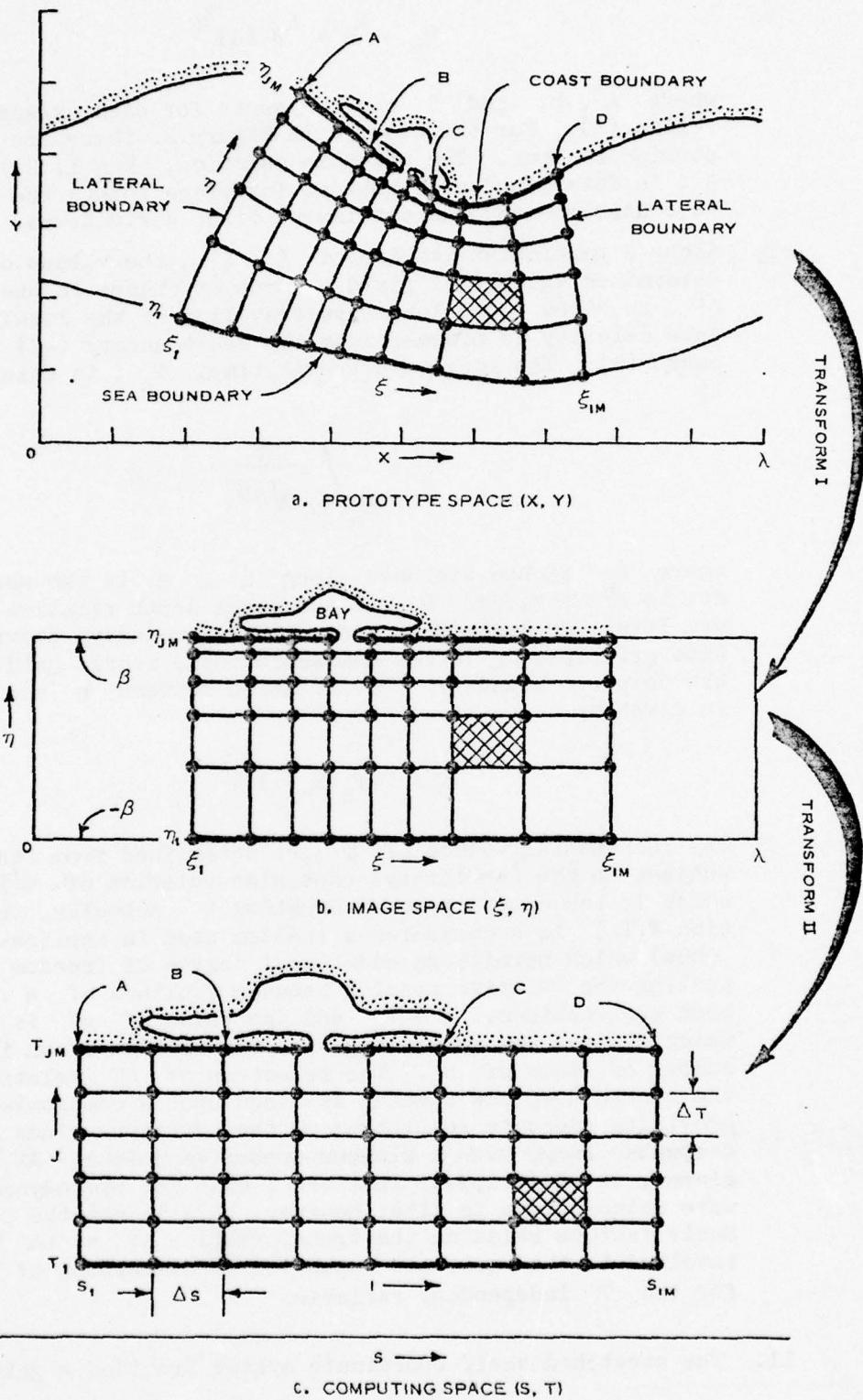
Figure 2.   Grid transformations for H computing grid

$$S_p = {}^kA + {}^kB \, (S)^{{}^kC} \tag{5}$$

where A , B, and C are constants for each expansion
region (k). For the example in Figure 2, there are three ex-
pansion regions. The ensemble function, k = 1, 2, and
3 , is determined such that at interface points the function
is continuous and has continuous first derivatives.

b. Along a particular isoline of ξ , $\xi^{\dagger}$, the values of η are
determined which will yield a constant change in the time,
ΔT , required for a long wave traveling at the local free
wave celerity to proceed from the sea boundary ($-\beta$) to the
coast (β). The long-wave travel time, T_n , is calculated
by

$$T_n = \int_{S_n(\eta)} \frac{ds}{\sqrt{gD_o}} \tag{6}$$

where S_n is the distance along $\xi^{\dagger}$, g is the acceleration
due to gravity, and D_o is the local depth relative to mean
sea level for a standard basin. This procedure provides a
fine grid spacing in the nearshore and a coarse grid near
the deep sea boundary. The relation between η and T
is given by

$$T = T(T_n(S_n(\eta))) \tag{7}$$

The incremental values of T are determined from Equation 6
subject to the (arbitrary) expansion relation of $T(T_n)$
which is the counterpart of Equation 5. Actually, the rela-
tion $T(T_n)$ is a convenience (seldom used in applica-
tions) which permits an additional degree of freedom in ad-
justing the relative spacing between isolines of η . In
most applications, $T = T_n$ and the value of ΔT is that
which divides the total long-wave travel time by an integer
number of lines of η . The selection of ΔT relative to
the coarse deep sea spacing is based upon a compromise for
providing adequate resolution of the hurricane winds and the
deepwater surge with a minimum number of points. At first
glance, it would appear that the T axis for hydrodynamic long-
wave calculations is time; however, this is not the case.
Scale factors relating the transformation of η to T are
involved in the equations resulting in dimensions of length
for the T independent variable.

11. The stretched shelf coordinate system provides a grid system

12

with a finer resolution near the coast than at the deep sea boundary.
The expansion curve, $S(S_p)$, stretches the alongshore reach of the grid
while maintaining a finer grid in the area of principal interest. In
this manner, an economy is achieved in terms of the number of grid points
required for long-wave simulation. However, because the preferred expansion curves dictate the locations (in prototype space) of the fluid
depths required for the long-wave calculations, the depth field must be
redefined for different combinations of stretching functions.

Governing Equations

12. The vertically integrated form of the quasi-linear long-wave
equations in a Cartesian system is well known.[1] The appropriate forms
of these equations in the stretched shelf coordinate system are

Transport (momentum) equations

$$\frac{\partial Q_S}{\partial t} - f Q_T + \frac{gD}{F\mu} \frac{\partial}{\partial S} (H - H_B) = \tau_S - \sigma_S \tag{8}$$

$$\frac{\partial Q_T}{\partial t} + f Q_S + \frac{gD}{F\nu} \frac{\partial}{\partial T} (H - H_B) = \tau_T - \sigma_T \tag{9}$$

and

Continuity equation

$$\frac{\partial H}{\partial t} + \frac{1}{F^2} \left[\frac{1}{\mu} \frac{\partial}{\partial S} (FQ_S) + \frac{1}{\nu} \frac{\partial}{\partial T} (FQ_T) \right] = 0 \tag{10}$$

where Q is the volume transport per unit width (units of length^2/time),
τ is the wind stress divided by water density, σ is the bottom
frictional resistance stress divided by water density, f is the
Coriolis parameter, g is the acceleration due to gravity, H is the
sea surface elevation relative to mean sea level, D is the total

13

instantaneous depth of water ($=H - D_o$), D_o the water depth relative to mean sea level, and H_B is the hydrostatic elevation of the sea surface corresponding to the atmospheric pressure anomaly. The independent variables are time (t) and the coordinates (S,T). The terms F, μ and ν are variable scale factors associated with the transformations. It can be shown that F is nondimensional and given by

$$F = \left[\left(\frac{\partial x}{\partial \xi} \right)^2 + \left(\frac{\partial y}{\partial \xi} \right)^2 \right]^{1/2} \tag{11}$$

The μ and ν scale factors are

$$\mu = \frac{\partial \xi}{\partial S_p} \frac{\partial S_p}{\partial S} \tag{12}$$

and

$$\nu = \frac{\partial \eta}{\partial S_n} \frac{\partial S_n}{\partial T_n} \frac{\partial T_n}{\partial T} \tag{13}$$

It can be shown that $\mu(\delta S)$ and $\nu(\delta T)$ have the dimensions of length. Furthermore, $F^2 \mu \nu$ corresponds to the Jacobian of the transformation in the sense that

$$A = \iint_R F^2 \mu \nu \ dS \ dT \tag{14}$$

where A is the area of a closed region in prototype space whose corresponding area in the computing space is R (see Figure 2 for details). This relation assures that all area enclosed by the limits of the curvilinear grid in prototype space is accounted for in the computing space by use of the scale factors.

13. The kinematic wind-stress components τ_S and τ_T are related to their x,y component counterparts (τ_x, τ_y) at a given point in prototype space by

$$\tau_S = \tau_x \cos \theta + \tau_y \sin \theta \tag{15}$$

and

$$\tau_T = -\tau_x \sin \theta + \tau_y \cos \theta \tag{16}$$

where

$$\theta = \tan^{-1} \left(\frac{\partial y / \partial \xi}{\partial x / \partial \xi} \right) \tag{17}$$

The relation between the wind stress and wind speed at a reference anemometer level (usually taken near the water surface) is taken as

$$\tau = K W_{10}^2 \ , \ K = \frac{\rho_a}{\rho_w} C_d \tag{18}$$

where ρ_a is air density and ρ_w is water density, C_d is a non-dimensional drag coefficient, and W_{10} is the wind speed at an elevation of 10 meters above the water surface. The value of K is taken as

$$K = \begin{cases} 1.1 \times 10^{-6} & , \text{ if } W_{10} \le 13.58 \text{ knots} \\[2em] \left[1.1 + 2.5 \left(1 - 13.58/W_{10} \right)^2 \right] 10^{-6} & , \text{ if } W_{10} > 13.58 \text{ knots} \end{cases} \tag{19}$$

This form for K was used in previous studies.[3,6] Recent compilation[7] of various results relating C_d to the wind speed at 10 meters is shown in Figure 3. As reference, the dashed line in Figure 3 shows the C_d relation based on Equation 19 with $\rho_a/\rho_w = 0.0012$. In the middle to low wind speed range (say, less than 60 knots), Equation 19 is representative of the data. It is this range of wind speeds that were used by Reid and Bodine[6] in studies of historical storm surges in Galveston Bay. Wanstrath[3], on the other hand, in studying three historical storm surges, each in different coastal regions, computed coastal water levels in good agreement with observed conditions using

15
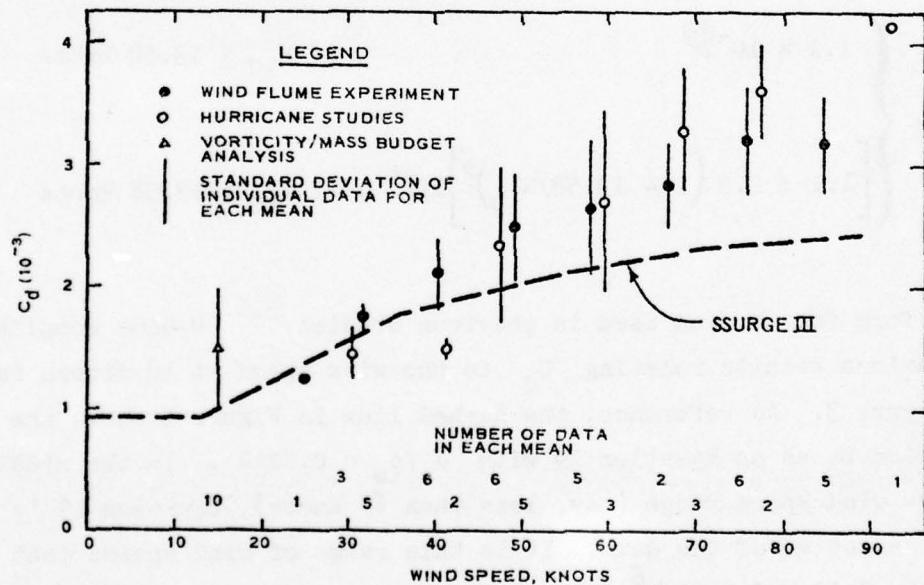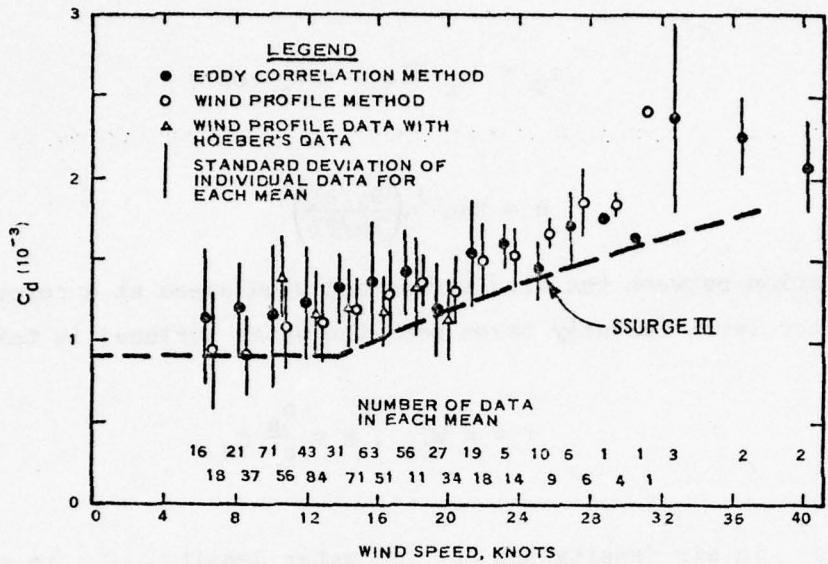
Figure 3. Mean values of the neutral drag coefficient as a function of low and high wind speeds at 10-m height (from Garratt, 1977) and that used in SSURGE III

Equation 19 and estimates of the wind furnished by the Hydrometeorological Section (Hydromet) of the National Weather Service (NWS), National Oceanic and Atmospheric Administration (NOAA). Those maximum winds ranged from 95 to 120 knots. However, the current understanding of the surface winds from hurricanes obtained by aerial reconnaissance, anemometer records from oil platforms, and sophisticated numerical marine boundary layer models[8,9] is that the surface winds at 10 meters are not as severe as thought. Consequently, with liberal estimates for the maximum winds, a conservative drag coefficient at high wind speeds is necessary. The procedure does provide good surge results as evidenced by these and previous studies. Actually, all previously reported open-coast surge models are subject to recalibration given the recent findings of hurricane surface winds.

14. The forms of the seabed frictional resistance terms are

$$\sigma_S = \frac{K_o Q}{D^2} Q_S \tag{20}$$

and

$$\sigma_T = \frac{K_o Q}{D^2} Q_T \tag{21}$$

where

$$Q = \left(Q_S^2 + Q_T^2 \right)^{1/2} \tag{22}$$

and K_o is a variable nondimensional drag coefficient that depends on the seabed condition and water depth. For typical seabed conditions,

$$K_o = \frac{g(0.025)^2}{(1.49)^2} (D^*)^{-1/3} \tag{23}$$

where

$$\begin{aligned}
D^* &= 0.25 \,, \text{ if } \quad\quad D < 0.5 \\
D^* &= 1.0 \,\,\, , \text{ if } 0.5 \leq D < 1.5 \\
D^* &= 2.0 \,\,\, , \text{ if } 1.5 \leq D < 2.5
\end{aligned} \tag{24}$$

and all depths D and D^* are in feet.

17

Recursion Equations

15. The numerical analogs of Equations 8-10 are based on centered difference approximations of all terms. The algorithm treats the time dependency explicitly and employs computing lattices as shown in Figure 4. The recursion equations require two time levels to complete the cycle. H values as well as H_B and τ are computed on the lattice at time level n. This lattice also contains the permanent storage data of D_o, θ, X_g, and Y_g where X_g and Y_g are the x and y grid coordinates of H points. For a reference index (I,J), the transports Q_S and Q_T are computed at $\Delta S/2$ and $\Delta T/2$, respectively, from the H point in the positive axes direction. The transports are computed on the lattice at time level $n+1$. For small time steps, Δt, it is inconsequential that τ is computed at n and applied at $n+1$. Furthermore, τ is computed at H point locations and averaged with its neighbor in the S and T directions, respectively, for determination of τ_S and τ_T. These approximations for τ are a result of efficient utilization of computer time and memory considerations and can be shown through numerical experiments to be accurate.

16. Consider that the transports are known at time level $n-1$ and the H field is known at time level $n-2$. The recursion formula for <u>interior</u> grid H points is

$$H(I,J,n) = H(I,J,n-2)$$

$$- \frac{2\Delta t \left[F_U(I,J)Q_S(I,J,n-1) - F_U(I-1,J)Q_S(I-1,J,n-1) \right]}{M_f \Delta S \mu_H(I) \left[F_H(I,J) \right]^2}$$

$$- \frac{2\Delta t \left[F_V(I,J)Q_T(I,J,n-1) - F_V(I,J-1)Q_T(I,J-1,n-1) \right]}{M_f \Delta T \nu_H(J) \left[F_H(I,J) \right]^2} \tag{25}$$

where I, J, and n indices express the S, T, and time

18
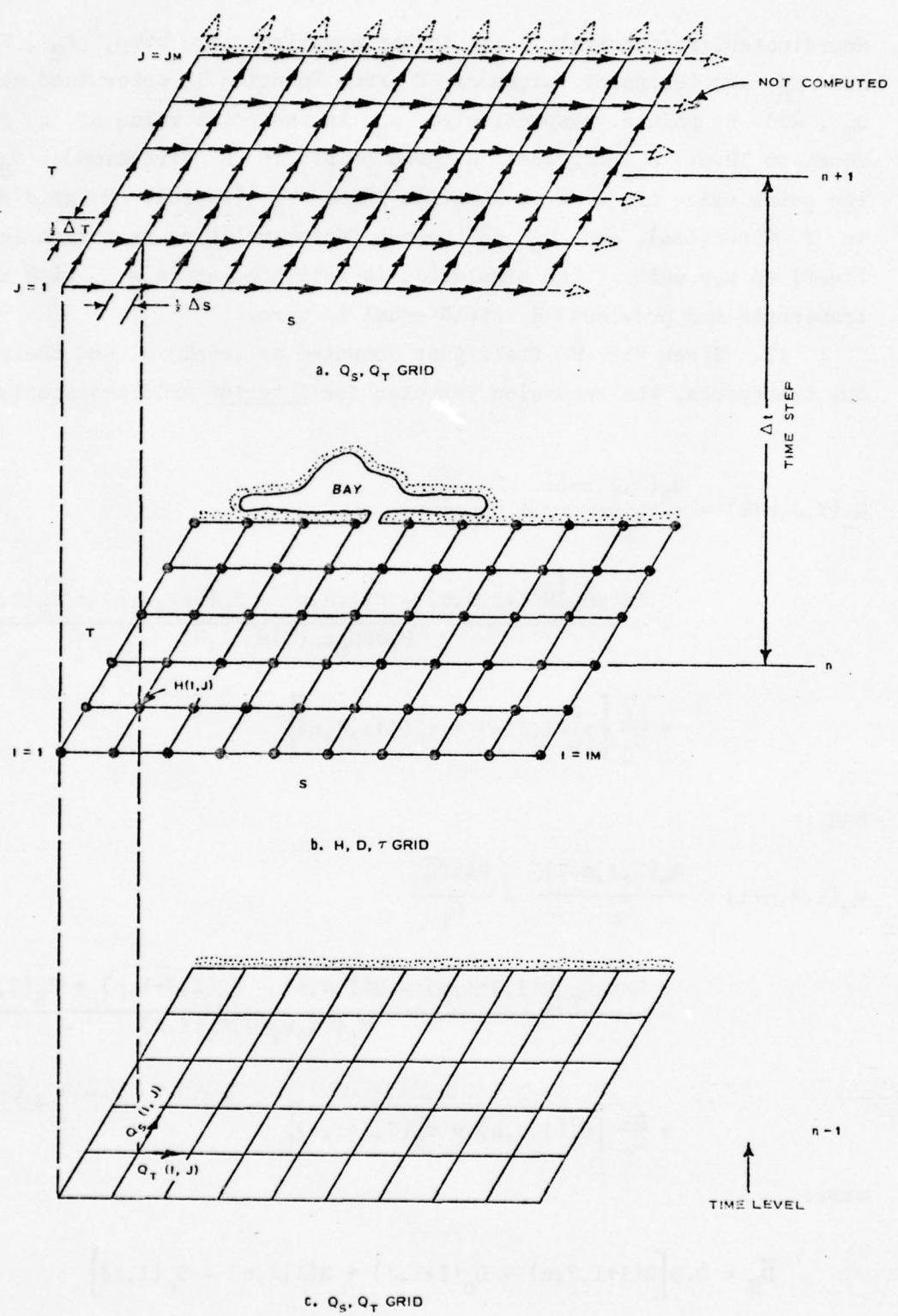
Figure 4. Time-dependent scheme for computed variables

19

coordinates, respectively, Δt is the numerical time step, F_U, F_V, and F_H are the point values of F from Equation 11 determined at Q_S, Q_T, and H points, respectively, μ_H is the point value of μ from Equation 12 at S_I (typical H grid points in S direction), ν_H is the point value of ν from Equation 13 at T_J (typical H grid points in T direction), and M_f is the map factor relating prototype length (feet) to x,y units. The simulation is initiated at $n = 1$ with all transports and previous H field equal to zero.

17. Given the H field just computed at level n and the previous transports, the recursion formulas for <u>interior</u> grid transports are

$$Q_S(I,J,n+1) = \frac{Q_S(I,J,n-1)}{G_S} + \frac{2\Delta t f \overline{Q}_T}{G_S}$$

$$- \frac{2\Delta t g \overline{D}_S \left[H(I+1,J,n) - H(I,J,n) - H_B(I+1,J,n) + H_B(I,J,n) \right]}{M_f \Delta S G_S \mu_U(I) F_U(I,J)}$$

$$+ \frac{\Delta t}{G_S} \left[\tau_S^H(I,J,n) + \tau_S^H(I+1,J,n) \right] \tag{26}$$

and

$$Q_T(I,J,n+1) = \frac{Q_T(I,J,n-1)}{G_T} - \frac{2\Delta t f \overline{Q}_S}{G_T}$$

$$- \frac{2\Delta t g \overline{D}_T \left[H(I,J+1,n) - H(I,J,n) - H_B(I,J+1,n) + H_B(I,J,n) \right]}{M_f \Delta T G_T \nu_V(J) F_V(I,J)}$$

$$+ \frac{\Delta t}{G_T} \left[\tau_T^H(I,J,n) + \tau_T^H(I,J+1,n) \right] \tag{27}$$

where

$$\overline{D}_S = 0.5 \left[H(I+1,J,n) - D_o(I+1,J) + H(I,J,n) - D_o(I,J) \right] \tag{28}$$

$$\overline{D}_T = 0.5\left[H(I,J+1,n) - D_o(I,J+1) + H(I,J,n) - D_o(I,J)\right] \tag{29}$$

$$\overline{Q}_S = \Big[0.25\, Q_S(I,J+1,n-1) + Q_S(I,J,n-1)$$

$$+ Q_S(I-1,J-1,n-1) + Q_S(I-1,J,n-1)\Big] \tag{30}$$

$$\overline{Q}_T = 0.25\Big[Q_T(I+1,J,n-1) + Q_T(I,J,n-1)$$

$$+ Q_T(I,J-1,n-1) + Q_T(I+1,J-1,n-1)\Big] \tag{31}$$

$$G_S = 1 + K_o^S \left\{ \left[Q_S(I,J,n-1)\right]^2 + \left(\overline{Q}_T\right)^2 \right\}^{1/2} \Big/ \left(\overline{D}_S\right)^2 \tag{32}$$

$$G_T = 1 + K_o^T \left\{ \left[Q_T(I,J,n-1)\right]^2 + \left(\overline{Q}_S\right)^2 \right\}^{1/2} \Big/ \left(\overline{D}_T\right)^2 \tag{33}$$

μ_U , in a similar manner, is the point value of μ from Equation 12 at $S_I + \Delta S/2$ (typical Q_S grid points in the S direction), ν_V is the point value of ν from Equation 13 at $T_J + \Delta T/2$ (typical Q_T grid points in the T direction), τ_S^H and τ_T^H are the wind stresses in the S, T directions, respectively, which are computed at H points, and K_o^S , K_o^T are the seabed drag coefficients computed from Equation 23 with D in Equation 24 given by $\overline{D}_S$ and $\overline{D}_T$, respectively.

Boundary Condition

18. For closure of the system of equations, the open sea and lateral boundaries require specification appropriate to the hurricane-induced surge computation. Many different continuum type boundary conditions are reported in the literature. In principle, it should

not matter which of these is used. If the computing grid is of suf-
ficiently large extent, the solution in the central part of the grid
near the coast should be insensitive to the particular one used. A
popular lateral boundary condition which is also used in SSURGE III
is

$$\frac{\partial Q_S}{\partial S} = 0 \qquad (34)$$

The sea boundary condition is that the water-surface elevation is placed
in equilibrium with the atmospheric pressure anomaly

$$H(I,1,n) = H_B(I,1,n) \qquad (35)$$

Along the lateral and sea boundaries, the transports are computed using
modified forms of Equations 30 and 31. The modification is to compute
an average value using only the two adjacent interior points.

19. It has long been recognized that the coast boundary condition
plays a major role in the nearshore hydrodynamic solution of the govern-
ing equations. Most open-coast shelf models (whether curvilinear,
rectilinear, finite element, implicit, or explicit) treat the coast as
an infinitely high, continuous wall. The use of numerical models in
simulating circulation and water level conditions is made difficult be-
cause of application of such a condition. The coast boundary condition
developed and incorporated into SSURGE III is the Finite Height Barrier
Coast (FHBC). The FHBC provides for the overtopping of low-lying land
and bay communication with the open sea.

20. The FHBC condition is to allow for potential ponding areas
landward of the shoreline. Figure 5 shows the conceptual design of the
barrier coast and adjacent bay. The bay is shown to be of several incre-
ments of ΔS in length. The coast flooding routine permits a volume of
water to be transported across the nominal shoreline which is dependent
upon barrier heights, predicted water level at the coast, channel en-
trance characteristics, and the water level in the ponding area, H_b .
The routine is applied at the H time levels as shown in Figure 4.

22
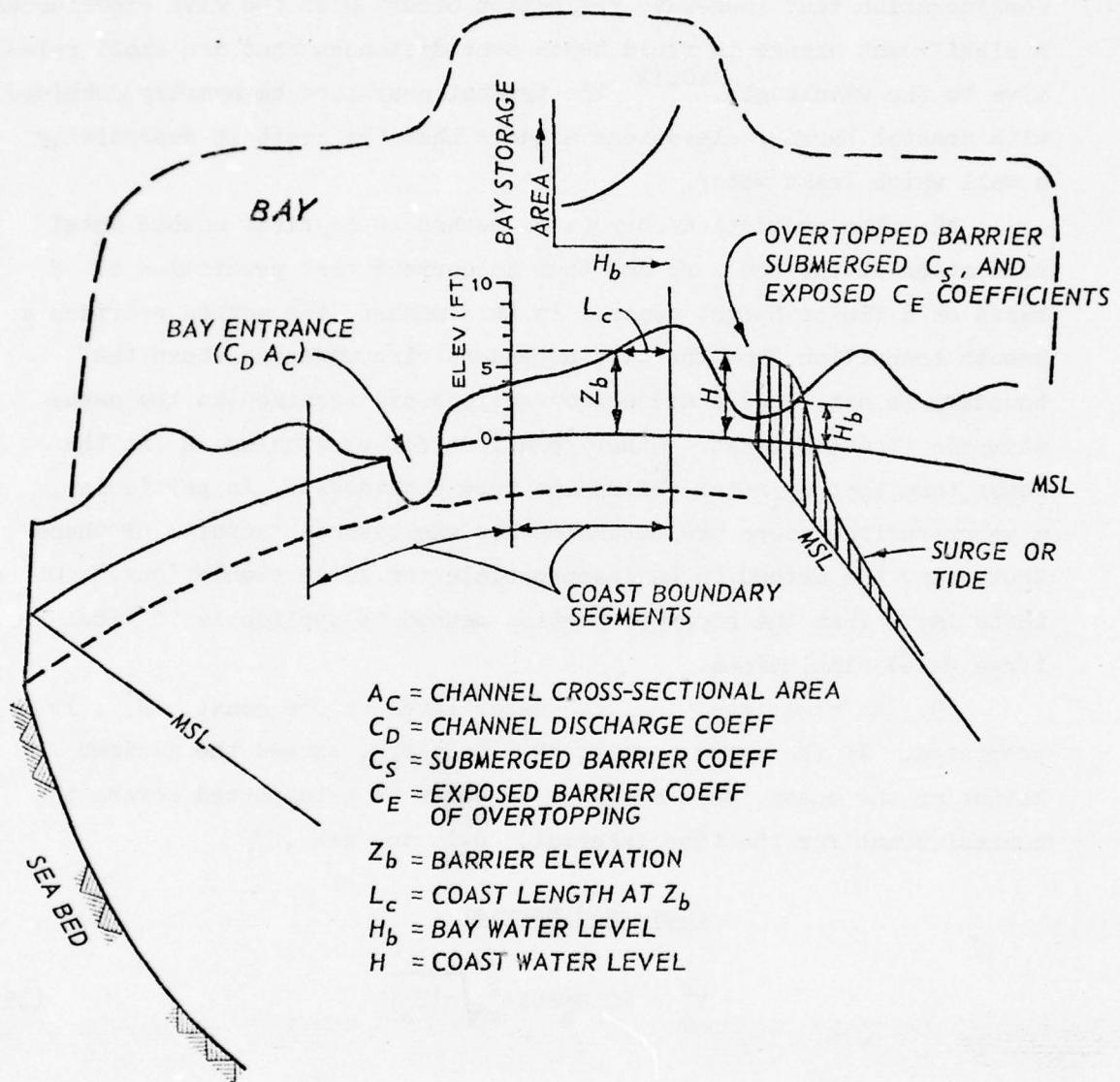
Figure 5. Finite height barrier coast boundary

A_C = CHANNEL CROSS-SECTIONAL AREA
C_D = CHANNEL DISCHARGE COEFF
C_S = SUBMERGED BARRIER COEFF
C_E = EXPOSED BARRIER COEFF OF OVERTOPPING
Z_b = BARRIER ELEVATION
L_c = COAST LENGTH AT Z_b
H_b = BAY WATER LEVEL
H = COAST WATER LEVEL

BAY

BAY STORAGE AREA

H_b

OVERTOPPED BARRIER SUBMERGED C_S, AND EXPOSED C_E COEFFICIENTS

BAY ENTRANCE ($C_D A_C$)

ELEV (FT)

L_c

Z_b

H

H_b

MSL

MSL

SURGE OR TIDE

COAST BOUNDARY SEGMENTS

MSL

SEA BED

23

21. A prediction/correction method is used to compute $H(I,JM,n)$.
The philosophy is taken that the coast barrier as viewed by the long wave
is essentially a wall over much of the time of surge development, re-
flecting the majority of the long-wave energy. This results from the
consideration that long-wave reflection occurs when the wave experiences
a significant change in fluid depth over distances that are small rela-
tive to the wavelength.[10,11] The typical nearshore bathymetry combined
with coastal barrier elevations assures that the coast is essentially
a wall which leaks water.

22. The prediction/correction method is to first assume total
reflection at the boundary and then to correct that prediction of H
based on a finite height coast. In this manner, the method provides a
smooth transition from the time-dependent circumstances where the
boundary is not flooded and no corrections are required to the cata-
strophic flooding coast. Other relations for predicting H at the
coast than that of total reflection were considered. In particular,
a water-surface slope projection method was tested. Results of these
tests show the method to be inappropriate for surge simulations.[5] Other
tests imply that the slope projection method is applicable to tidal
(free wave) simulations.

23. At time level n , the water level at the coast, H^+ , is
predicted. If the water levels, H^+ and H_b , exceed the minimum
height of the coast, then a volume of water is transported across the
nominal coast for the time interval, n-1 to n+1 ,

Submerged barrier

$$V_A^k = 2C_S D_h \Delta t \Delta L_c^k \sqrt{g|D_h|} \tag{35}$$

where

$$D_h = H^+ - H_b \tag{36}$$

$$\Delta L_c^k = |L_c^k - L_c^{k+1}| \tag{37}$$

24

C_S is a nondimensional submerged barrier coefficient taken as 0.4, L_c^k and L_c^{k+1} are lengths of the coast at elevations Z_b^k and Z_b^{k+1}, respectively, and the direction of the flow is determined by the sign of D_h (positive means water is removed from the coastal cell and placed in the ponding area). Barrier heights per ΔS section centered on H points are discretized into unit elevations (k). The length of the coast at each elevation is obtained from topographic maps, beach surveys, etc. The total volume of water crossing the submerged coast is the summation of Equation 35 for $k = 0$, $1...K$ where K is the integer of the lesser of H^+ or H_b. Considering large ponding areas and high minimum coastal heights, this volume is generally small compared with that which is transported through channels or which over-topped the exposed (on one side) section of the barrier. These submerged barrier equations reflect the assumption that frictional effects are dominant in the bottom layer which is continuous across the boundary.

24. For the overtopped barrier, the volume of water crossing the coast is

Exposed (on one side) barrier

$$V_B^k = 2C_E D_b^k \Delta t \Delta L_c^k \sqrt{g|D_b^k|} \tag{38}$$

where

$$D_b^k = \begin{cases} Z_b^k - H_b, & \text{if } H^+ < Z_b^k < H_b \\ \\ H^+ - Z_b^k, & \text{if } H_b < Z_b^k \leq H^+ \end{cases} \tag{39}$$

C_E is a nondimensional exposed barrier coefficient taken as 0.2 and the direction of flow is determined by the sign of D_b. The total volume of water overtopping the coast is the summation of Equation 38 for $k = 0,1,...M$ where M is the integer of the greater of H^+ or H_b.

25

25. The volume of water associated with channel communication is

$$V_C = \pm\ 2\Delta t\ \ C_D A_c\ \ \sqrt{g|H^+ - H_b|}\ + W_c D_c\ \sqrt{gD_c} \qquad (40)$$

where

$$D_c = \begin{cases} |H^+ - H_b| & , \text{ if } H^+ > 0 \text{ and } H_b > 0 \\ H^+ & , \text{ if } H^+ > 0 \text{ and } H_b < 0 \\ H_b & , \text{ if } H^+ < 0 \text{ and } H_b > 0 \\ 0. & , \text{ if } H^+ < 0 \text{ and } H_b < 0 \end{cases} \qquad (41)$$

W_c is the channel width, C_D is a nondimensional channel discharge coefficient determined for each entrance, A_c is the channel cross-sectional area at mean sea level, and the sense of the flow is taken toward the low head side. An estimate of $C_D A_c$ is possible if tidal observations are available inside and outside a bay with a constricted opening to the sea

$$C_D A_c = \frac{A_s}{T}\sqrt{\frac{32\pi H_o}{3gB_p}} \qquad (42)$$

where A_s is the surface area of the bay at mean sea level, T is the tidal period, H_o is the tidal range outside the bay, and B_p is a nondimensional bay parameter that is dependent on the response (H_o/H_i) or phase lag. H_i is the tidal range inside the bay. The bay parameter as a function of response or phase lag is shown in Figure 6.[12]

26. Consider that H^+ values along the coast (uncorrected for flooding) are known at time level n and H_b and A_b are known at level $n-2$ where A_b is the bay storage area. The volume of water entering (or leaving) the ponding area is determined for each segment by the appropriate sum of V_A^k, V_B^k, and V_C. The ratio of that volume to the surface area of the grid block representative of H^+, A_I, provides the incremental correction to the predicted coastal water level to conserve mass. This value is stored in $H(I,JM,n)$ for use in

26
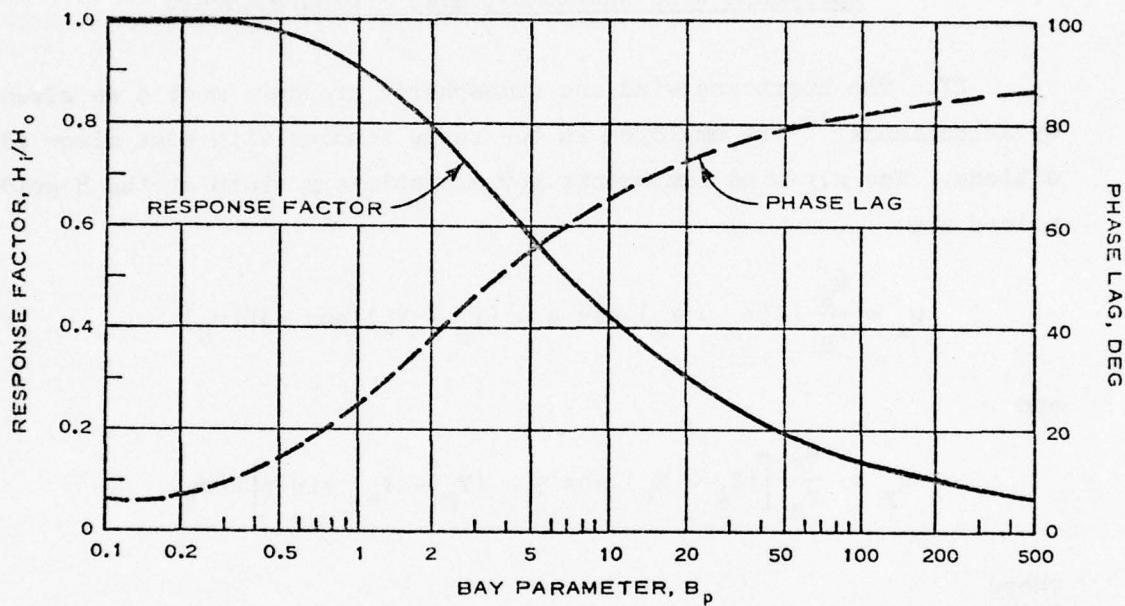
NOTE: H_i = TIDAL RANGE
INSIDE THE BAY

H_o = TIDAL RANGE
OUTSIDE THE BAY

Figure 6. Bay parameter B_p as a function of response factor
or phase lag

27

the <u>transport</u> <u>computations</u> <u>at</u> <u>level</u> <u>n+1.</u> The new value of H_b at
time level n is H_b at $n-2$ plus the incremental water-level change
from the instantaneous and even distribution of the entering volume
(the sum for all appropriate ΔS segments) on A_b at level $n-2$.
From H_b at n , a new bay storage area is obtained. The above is
repeated for each ponding area and its designated coastal segments.

Hurricane Wind and Atmospheric Pressure Models

27. The hurricane wind and atmospheric pressure models as given
by Jelesnianski[13] are employed in the surge studies with some minor ad-
ditions. The x,y-wind components for a stationary storm at the H grid
points are

$$w_x = \frac{W_R}{r_H}\,[-(X_g - X_e)\,\sin\phi - (Y_g - Y_e)\,\cos\phi]F(r_H) \tag{43}$$

and

$$w_y = \frac{W_R}{r_H}\left[(X_g - X_e)\,\cos\phi - (Y_g - Y_e)\,\sin\phi\right]F(r_H)$$

where

$$r_H = [(X_g - X_e)^2 + (Y_g - Y_e)^2]^{1/2} \tag{44}$$

$$F(r_H) = \begin{cases} \left(\dfrac{r_H}{R_H}\right)^{3/2} & \text{, if } r_H < R_H \\[2ex] \left(\dfrac{R_H}{r_H}\right)^{1/2} & \text{, if } r_H \geq R_H \end{cases} \tag{45}$$

W_R is the stationary storm maximum wind, ϕ is the wind ingress angle
reflecting the inward flow relative to that wind vector tangent to the
isovel, R_H is the distance from the storm center (X_e, Y_e) to region of
maximum winds, and X_g and Y_g are the (x,y) coordinates of H grid

points. The translation of the storm provides an alteration in the wind field. The x,y supplemental wind components due to storm translation are

$$t_x = (T_x \cos \psi + T_y \sin \psi)G(r_H) \tag{46}$$

and

$$t_y = (-T_x \sin \psi + T_y \cos \psi)G(r_H) \tag{47}$$

where

$$\psi = \alpha - \phi - 90 \tag{48}$$

$$G(r_H) = \begin{cases} \dfrac{r_H}{r_H + R_H} & , \text{ if } r_H < R_H \\ \\ \dfrac{R_H}{R_H + r_H} & , \text{ if } r_H \geq R_H \end{cases} \tag{49}$$

T_x and T_y are x,y components of the forward speed of the storm and α is a rotation angle used, primarily, to fine tune the alignment of maximum winds. For standard operation of the wind model, α is set equal to $90° + \phi$. The x,y-wind stress components for a moving storm are

$$\tau_x = K \left(w_x^2 + w_y^2 \right)^{1/2} W_x \tag{50}$$

and

$$\tau_y = K \left(w_x^2 + w_y^2 \right)^{1/2} W_y \tag{51}$$

where

$$W_x = w_x + t_x \tag{52}$$

$$W_y = w_y + t_y \tag{53}$$

29

and K is given by Equation 19. The stress components in the stretched shelf coordinate system are determined by applying Equations 50 and 51 in Equations 15 and 16. In an alternate manner,

$$W_S = W_x \cos \theta + W_y \sin \theta \tag{54}$$

and

$$W_T = -W_x \sin \theta + W_y \cos \theta \tag{55}$$

where θ is given by Equation 17 and W_S and W_T are the wind components in the (S,T) system. The stress components are

$$\tau_S = K \left(W_S^2 + W_T^2 \right)^{1/2} W_S \tag{56}$$

and

$$\tau_T = K \left(W_S^2 + W_T^2 \right)^{1/2} W_T \tag{57}$$

28. The surface atmospheric pressure field associated (but not dynamically coupled) with the hurricane wind is

$$P = P_o + (P_\infty - P_o)e^{-R_H/r_H} \tag{58}$$

where P_o is the central pressure and P_∞ is the far-field pressure. It is often observed that relatively high winds remain along the coast after the storm has proceeded inland. Through numerical experiments, it is found that reasonably good comparison between observed (Hydromet) and computed winds is obtained by setting R_H to be the distance the storm center is from the coast, specifying W_R to be desired winds at the coast and setting α (measured clockwise from the storm movement) such that the maximum wind region is along the coast. This procedure allows slightly longer simulations to be performed after landfall than would be permitted otherwise due to poor wind-field portrayal. However, R_H in the pressure expression (Equation 58) is not allowed to increase.

30

If this procedure is followed in the numerical program (it is optional), R_H is held constant at a value RHIT in nautical miles (n.mi.) after the time of storm landfall (THIT) which is input in hours after the start of the simulation.

29. The various program parameters that are used to generate the wind and atmospheric pressure fields for Hurricanes Flossy,[14] Hilda,[15] Betsy,[16] and Carmen are given in Tables 1-4. Only for the postlandfall winds from Hurricanes Hilda, Betsy, and Carmen were the normal routines modified in the above manner. This is seen by noting the number for THIT. For comparison, the computed and observed (Hydromet) wind field at selected times are presented in Plates 1-3 for Hurricane Hilda and in Plates 4-6 for Hurricane Betsy.

30. The term H_B in Equations 8, 9, 26, 27, and 35 is computed in feet of water by

$$H_B = 0.0328(P_\infty - P) \tag{59}$$

where P_∞, named PINF in Tables 1-4, and P_O are in pressures of millibars.

31. For historical storms, all _necessary_ input parameters can be determined if Hydromet has assessed the maximum winds W_R following the same procedures. This procedure probably results in a liberal esti- mate for W_R. Storm surge simulations for forecasting purposes typi- cally involve storm parameters of track, P_∞, P_O, and R_H. The only other necessary input for this wind model is W_R. This can be determined from the correlation of a few severe historical storms where Hydromet has estimated W_R and that value which is predicted by the Standard Project Hurricane (SPH) method[17] using only the required fore- cast storm parameters. A cursory examination shows that the ratio W_R to W_{max}(SPH) is probably in the range 1.2 to 1.3. This approach is suggested only as a temporary solution. Actually, a dynamic marine boundary layer hurricane model is needed that is independently cali- brated to several storms of record and verified against even more historical storms. This wind model is comparable to the treatment of the physics of the atmosphere as SSURGE III is to the hydrodynamics.

31

PART IV: HURRICANES FLOSSY, HILDA, BETSY, AND CARMEN
SURGE STUDY

32. Hurricanes Flossy, Hilda, Betsy, and Carmen affected the
Louisiana coast from Atchafalaya Bay to the Mississippi River.
Hurricane Flossy is the only storm in this study that paralleled this
coastal region with subsequent landfall near Pensacola, Fla. Plate 7
shows the location map, the four storm tracks, and the computing grid.
The Mississippi River delta region and the adjacent levees are simulated
as nonovertopping barriers protruding from the coast in the manner shown
in Plate 7. For three of these hurricanes, Hydromet has estimated
the surface wind fields at various storm locations.[14,15,16] Information
about Hurricane Carmen is from personal communication with Dr. Joe
Pellissier, National Hurricane Center (NHC), NOAA, Miami, Fla. It is
noted that the storm tracks as observed from Hydromet, other weather
bureau offices as noted in poststorm damage survey reports of the U. S.
Army Engineer District, New Orleans (NOD), and from the NHC in-house
historical storm track record are, in most cases, somewhat different--
in particular, the track of Hurricane Flossy as it crossed the
Mississippi River delta and Hurricane Carmen as it approached Lake
Charles, La., in which the storm was decaying (filling) rapidly. The
storm tracks presented in this report are from the NHC record except
that the track of Hurricane Hilda prior to landfall is moved 6 n.mi.
to the east and the track of Hurricane Flossy in the Mississippi
River region is a compromise between the NOD report and NHC.

33. Six discrete ponding areas with storage area information and
FHBC data are presented in Table 5. Flood Region I is from Marsh Is.
to Point Au Fer Is. and bounded inland by elevated railroads or highways,
spoil banks of canals, bayous, or other waterways. Flood Region II
is from the terminal point of Flood Region I to Wine Is. and bounded
inland by the spoil banks of the Houma Navigation Canal to the east and
Bayou Chene to the west and highway U.S. 90 to the north. Flood
Region III is from Wine Is. to Belle Pass and bounded inland by the
Houma Navigation Canal, Bayou Lafourche to the east, and Bayou Blue and

32

a portion of U.S. 90 to the north. Flood Region IV is from Belle Pass to Barataria Pass and bounded inland by Bayou Lafourche, Barataria Bay Waterway, and U.S. 90 to the north. Flood Region V is from Barataria Pass to the west bank of the Mississippi River levee and bounded inland by the Barataria Bay Waterway which closes with the levee near New Orleans, La. Flood Region VI is from the east bank of the Mississippi River levee to the entrance of Lake Borgne following the seaward extent of the marsh area and bounded inland by New Orleans and U.S. 90. All the above-mentioned bayous, canals, etc., have spoil or natural alluvial banks associated with them that would have the tendency to limit flows from one flood region to another.

34. For Hurricane Flossy which occurred in September 1956, the coastal surge envelope for a wall and flooding coast boundary conditions is presented in Plate 8. The comparison of computed water-level envelope and observed high-water conditions is presented in Table 6 for coastal areas. Table 7 shows the peak value of H_b and the observed conditions for each flood region. The observed conditions are taken from the NOD poststorm survey[18] which is presented in Plate 9. The comparison of computed and observed conditions is not as good as should be expected.

35. The term "coastal surge envelope" refers to the peak surge water elevations along the coast without regard to the time of its occurrence. Whereas, the computed coastal water-level envelope is the peak water level from the time-record made by the superposition of the expected tide and the surge hydrographs at a particular location without regard to the time of its occurrence. It is more difficult to compare computed H_b and observed inland high-water levels because the tide cannot be simply added to the computed surge. Furthermore, H_b loses some meaning in surge simulations where for inland locations, the local wind setup is of major importance. Consider a surge of 5 ft occurring at a time of low tide which is expected to be -5 ft relative to msl. The surge model would compute flooding relative to barrier elevations based on msl and surge levels (rel msl). The result is an erroneous computation for H_b and, to a lesser degree, also for the coastal

surge. However, for small tide ranges such as exist in the Gulf of
Mexico, the computations for the open-coast water level are representa-
tive of the superposition of tide and surge. This problem can be, in
general, avoided if the tide function is input at the sea boundary and
dynamically computed along with the surge. It is recommended that this
should be pursued when a generalized predictive tide function appropri-
ate to the edge of he continental shelf becomes available.

36. Hurricane Hilda occurred in October 1964. Plates 10-15
show the water-surface topography together with the depth-averaged
velocity field for a wall and flooding coast boundary in 6-hr intervals
over a 30-hr period. The role of the Mississippi River delta in limit-
ing the free transport in the continental shelf waters is clearly seen
in the series of the above snapshots. The effect of a flooding boundary
relative to a wall is seen to enhance the onshore-directed transport of
water in the nearshore and not-so-nearshore region. This would result
in more sea sediment and suspended material transported to (and over)
the coast than that computed in nonflooding open-coast models. The
principal surge area occurs at Caillou Bay as seen in Plates 12 and 16,
which show the surge envelopes. The coastal barrier in this area is
typically a beach berm, generally less than 3 ft in height (msl). Con-
sequently, significant flooding occurred from 1800Z (Z referring to
Greenwich Mean Time), 3 October, to approximately 0300Z the next day.
The winds at 0300Z, 4 October, are directed more alongshore, forcing
the inland surge to the east. The highest observed water level of
9.8 ft occurred inland, to the east of Caillou Bay along the Houma
Navigation Canal. It is seen that the difference in surge envelopes
for a wall and flooding coast conditions (Plate 16) is at most 2 to
3 ft. This difference, although seemingly small, reflects a significant
flooding condition. In proper perspective, the volume of water flood-
ing the coast is inconsequential to that volume entrained in the near-
shore open-sea circulation. Consequently, water can be removed from
the coast and be almost instantaneously replaced without significant
effect on the nearshore water level. The circulation pattern, however,
is greatly changed due to the flooding.

34

37.   Tables 8 and 9 compare the computed and observed high-water levels for coastal and inland regions, respectively. The observed water-level record and that computed (superposition of surge and expected tide as determined from the National Ocean Survey tide table) at various coastal locations are presented in Plates 17-19. An oscillation of 8 hr in period is shown in the computed hydrograph at Biloxi, Miss. (Plate 19). The period of oscillation is characteristic of an edge wave. Multioscillations occur from the trapping of energy between the right lateral boundary and the protruding Mississippi River levee. However, other computed water levels in this region do not exhibit such oscillations as shown in Plates 18 and 20. Plate 17 shows another typical problem in open-coast surge computations--that of proper wind specification. Before storm landfall, the analytically computed winds at Eugene Is. are always directed offshore, resulting in the enhanced drawdown of the water. Moreover, the island is on the leeward side of the coast and land frictional influence on the wind is not considered in the hurricane model. Further complication occurs in light of recent developments which shows that the surface winds in the forward section of the storm may be outflowing (a negative ingress angle).[19] The results presented in the comparison tables and in Plates 17-19 are in good agreement with the observed; however, improvement should be expected with a better wind model. Plate 21 presents the observed high-water levels as reported in the poststorm survey.[20]

38. Hurricane Betsy occurred in September 1965. The water-surface topography and velocity field comparing a wall and flooding coast boundary are shown in Plates 22-26. The effects of the flooding boundary on the nearshore water levels and currents are most dramatically demonstrated in Plate 23. Without overtopping, the wall condition is trapping water in excess of 18 ft at the corner between the east Mississippi levee and coastal wall. With flooding of the marsh area, only 12 ft of water is computed along the levee. The coastal surge envelope (Plate 27) clearly shows the effect of a flooding boundary versus that with a wall. The velocity fields are considerably different with, again, the enhancement of the onshore velocity for the flooding

35

boundary. Plate 23 also shows that the surge is just beginning to develop on the western side of the Mississippi River levee. Plate 24, 3 hr later than that snapshot in Plate 23, shows the developed surge in this area while to the east, sustained relatively high water is continuing. Plates 25 and 26 show the decreasing surge and the reentrance of the water from the ponding areas.

39. Tables 10 and 11 compare the computed and observed high-water levels for coastal and inland regions, respectively. Furthermore, observed and computed hydrographs at two coastal locations are presented in Plates 28 and 29. The hydrograph location in Plate 28 is to the left of landfall. The problems associated with the computed large drawdown have been discussed previously. No presurge water-level anomaly is added to any of the computed results in any study reported herein, although after viewing the observed hydrograph at Biloxi, it may seem appropriate. The results from this surge simulation, more than in any other presented in this report, show the necessity in treating the coast as a finite barrier. The comparison of the computed and observed water-level conditions are in excellent accord. Plate 30 presents the observed high-water levels as reported in the poststorm survey.[21]

40. Hurricane Carmen occurred in September 1974. Snapshots of the water-surface topography, together with the depth-averaged velocity field for a wall and flooding coast, are shown in Plates 31-33. The principal surge developed between Caillou Bay and the entrance to Terrebonne Bay, as shown in the surge envelope (Plate 34), at approximately 0900Z, 8 September (between the time of Plates 31 and 32). The surge does not develop in Atchafalaya Bay until 1800Z. After this time, the forward motion and location of the storm are in question due to its rapid decay. Since the surge developed in East Cote Blanche Bay during the decay stage of the storm, it is viewed as fortuitous that the peak computed and observed water levels are in good agreement (Plate 35). The phasing of the peak water levels at Luke's Landing, La., is in poor agreement probably due to the storm proceeding faster on the track than that used in the simulation.

41. Plates 36-38 present computed and observed hydrographs at

36

other coastal locations. The observed hydrographs in the region to the east of the Mississippi River (Plates 37 and 38) show a considerable initial water elevation at the start of computations. This elevation is not totally a presurge condition because the action of the wind is seen to reflect the observed peak levels some 20 hr later. On the other hand, this initial condition, especially at the Gulf Outlet Canal, is not due to the hurricane since the winds on the continental shelf are very weak at the start of computations; that is, if the surge simulation had begun at 1200Z, 6 September (24 hr in advance of the starting time in Plate 76), the model would not have shown over 4 ft of water at the canal entrance at 1200Z, 7 September. Other processes are occurring, presumably not assignable to the storm surge, for whatever caused the transient water-level bump at 1700Z, 7 September (Plate 37) is probably responsible for a similar, well-correlated bump at 2200Z, 7 September, at Biloxi (Plate 38).

42. Tables 12 and 13 compare the computed and observed high-water levels for coastal and inland regions, respectively. There are no observations along the coast in the principal surge area for comparison with the computed value. In other places and subject to the above discussion, the comparison between computed and observed water levels is in good agreement. Plate 39 presents the observed high-water levels as reported in the poststorm survey.[22]

PART V: CONCLUSIONS AND RECOMMENDATIONS

43.   The development of a two-dimensional, time-dependent, curvilinear, open-coast storm surge model is presented. In particular, the model treats the coast boundary as a finite height barrier which is broken with bay entrances. The flooding coast routine in its treatment of submerged and exposed (on one side) barriers is considered conservative.

44.   Results of four storm surge simulations are presented in which observed and computed conditions are compared. Model results compare most favorably with those observed. The finite height barrier approach does indeed improve the hydrodynamic model's behavior in the nearshore region of the open coast but does not prove an accurate presentation of inland flooding levels where local wind setup is of major importance. Other techniques are required utilizing the results from the open-coast model for accurate modeling of inland flooding processes. From currently available data, a relatively low value for the wind drag coefficient at high wind speeds is used. This is necessary to compensate for the liberal estimate for the maximum winds. In hindcasting situations, it is not guaranteed that the same procedure is used for estimating the maximum wind. The wind model employed in these surge simulations from historical storms requires input of the maximum wind. The problem can be resolved by using a wind model based on the physics of the marine boundary layer that will provide a wind field as a result of dynamic meteorological computations. It is recommended that such a model be obtained (as they do exist) and incorporated into the hydrodynamic flooding coast model. The resulting composite model, therefore, would be appropriate for both forecasting and hindcasting and involve a drag coefficient reflective of the currently available data.

45.   The following recommendations are secondary to that of incorporating a dynamic wind model in SSURGE III. It can be shown that the astronomical tide does distort the predicted coastal and inland floodwater levels when it is not incorporated into the dynamic computations; that is, equivalent results are not obtained by the superposition of

38

surge and tide and that simulation where the tide is included in the sea boundary forcing condition. For the east coast of the United States where there are some locations with large tidal ranges, the tide should be included in the computation. The results of the four storm surge simulations performed for this study are considered sufficiently accurate using superposition of surge and tide since they occurred in Gulf of Mexico waters where the tidal range is small. It is recommended that a generalized tide prediction function which is appropriate to the edge of the continental shelf be incorporated into the surge computations.

46. It is recognized that other approaches, equations and coefficients are reported or can be developed for the treatment of a flooding, finite height barrier coast. These should be investigated and the more promising approach tested against the one reported herein.

REFERENCES

1. Welander, P., "Numerical Prediction of Storm Surges," _Advances in Geophysics,_ Vol 8, Academic Press, New York, 1961.

2. Jelesnianski, C. P., "A Sheared Coordinate System for Storm Surge Equations of Motion with a Mildly Curved Coast," Technical Memorandum NWS TDL-61, Jul 1976, Techniques Development Laboratory, National Oceanic and Atmospheric Administration, Silver Spring, Md.

3. Wanstrath, J. J. et al., "Storm Surge Simulation in Transformed Coordinates; Vol 1: Theory and Application," Technical Report 76-3, Nov 1976, U. S. Army Coastal Engineering Research Center, Fort Belvoir, Va.

4. Wang, J. D. and Connor, J. J., "Mathematical Modeling of Near Coastal Circulation," Report No. 200, Apr 1975, Ralph M. Parsons Laboratory, Department of Civil Engineering, Massachusetts Institute of Technology, Cambridge, Mass.

5. Wanstrath, J. J., "Nearshore Numerical Storm Surge and Tidal Simulation," Technical Report H-77-17, Sep 1977, U. S. Army Engineer Waterways Experiment Station, CE, Vicksburg, Miss.

6. Reid, R. O. and Bodine, B. R., "Numerical Model for Storm Surges in Galveston Bay," _Journal, Waterways and Harbor Division, American Society of Civil Engineering,_ Vol 94, No. WW1, Feb 1968, pp 33-57.

7. Garratt, J. R., "Review of Drag Coefficients over Oceans and Continents," _Monthly Weather Review,_ Vol 105, Jul 1977, pp 915-929.

8. Cardone, V. J. and Ross, D., "Forecasting Hurricane Winds and Waves--A Pilot Study," Final Report, 1976, Institute of Marine and Atmospheric Sciences, City University of New York, New York, N. Y.

9. Cardone, V. J., Pierson, W. J., and Ward, E. C., "Hindcasting the Directional Spectrum of Hurricane Generated Waves," _Journal, Petroleum Technology,_ Vol 28, Apr 1976, pp 385-394.

10. Wanstrath, J. J., _Reflection and Transmission of a Monochromatic Gravity Wave at Oblique Incidence to a Step,_ M.S. Thesis, Texas A&M University, College Station, Tex., 1971.

11. Cochrane, J. D. and Arthur, R. S., "Reflections of Tsunamis," _Journal, Marine Research,_ Vol 7, No. 3, 1948, pp 239-251.

12. Love, R. W., _Tidal Response of a Bay with a Constricted Opening to the Sea,_ M.S. Thesis, Texas A&M University, College Station, Tex., 1959.

13. Jelesnianski, C. P., "A Numerical Calculation of Storm Tides Induced by a Tropical Storm Impinging on a Continental Shelf," _Monthly Weather Review,_ Vol 93, 1965, pp 343-358.

14. Environmental Science Services Administration, "Pressure and Winds over the Gulf of Mexico in Hurricane Flossy, September 23-24, 1956," Memorandum HUR 7-53, Jun 19, 1958, U. S. Department of Commerce, Weather Bureau, Hydrometeorological Section, Washington, D. C.

15. _____, "Preliminary Analysis of Surface Winds in Hurricane Hilda, October 2-4, 1964," Memorandum HUR 7-82, Jun 8, 1965, U. S. Department of Commerce, Weather Bureau, Hydrometeorological Branch, Washington, D. C.

16. _____, "Surface Winds (30 ft) over the Gulf of Mexico in Hurricane Betsy, September 9 and 10, 1965," Memorandum HUR 7-87, Dec 20, 1965, U. S. Department of Commerce, Weather Bureau, Hydrometeorological Branch, Washington, D. C.

17. National Oceanic and Atmospheric Administration, "Revised Standard Project Hurricane Criteria for the Atlantic and Gulf Coasts," Memorandum HUR 7-120, Jun 1972, U. S. Department of Commerce, National Weather Service, Hydrometeorological Branch, Washington, D. C.

18. U. S. Army Engineer District, New Orleans, "Report on Hurricane Flossy--23-24 September 1956, Southeastern Louisiana," Aug 1957, New Orleans, La.

19. Shea, D. J. and Gray, W. M., "The Hurricanes Inner Core Region I, Symmetric and Asymmetric Structure," Journal, Atmospheric Science, Vol 30, 1973, pp 1544-1564.

20. U. S. Army Engineer District, New Orleans, "Report on Hurricane Hilda, 3-5 October 1964," May 1966, New Orleans, La.

21. _____, "Report on Hurricane Betsy, September 8-11, 1965," Nov 1965, New Orleans, La.

22. _____, "Report on Hurricane Carmen, 7-8 September 1974," Oct 1975, New Orleans, La.

Table 1

Program SSURGE III Wind Data for Hurricane Flossy Surge Simulation

PHI = 25.0
THIT = 9999.
RHIT = 9999.
PINF = 1014.56

Program Time (hrs)	Track Location				Rotation (°)	Radius To Maximum Wind (n. mi.)	Stationary Storm Maximum Wind (Knots)	Central Pressure (mb)
	Lat. (°N)	Long. (°W)	X_e	Y_e				
0*	25°50.2'	90°59.8'	282.2	-196.5	115.0	22.0	60.0	984.0
6	27°9.3'	90°54.5'	290.1	-69.5	115.0	22.0	60.0	984.0
12	27°58.8'	90°34.5'	318.0	8.5	115.0	22.0	60.0	984.0
15	28°22.9'	90°12.3'	349.0	46.5	115.0	22.0	65.0	982.0
18	28°44.8'	89°48.5'	382.0	81.5	115.0	22.0	70.0	979.0
21	29°4.0'	89°25.6'	414.0	112.0	115.0	22.0	75.0	975.0
24	29°21.5'	89°3.3'	445.0	140.0	115.0	22.0	75.0	975.0
27	29°41.6'	88°31.9'	489.0	172.5	115.0	22.0	75.0	974.0
30	29°48.0'	87°39.1'	562.0	182.5	115.0	22.0	75.0	974.0

* Program Time of 0 hrs = 1230 GMT, 23 Sept 1959.

Table 2

Program SSURGE III Wind Data for Hurricane Hilda Surge Simulation

PHI = 25.0
THIT = 23.0
RHIT = 24.0
PINF = 1014.56

| Program Time (hrs) | Track Location | | | | Rotation (°) | Radius To Maximum Wind (n. mi.) | Stationary Storm Maximum Wind (Knots) | Central Pressure (mb) |
	Lat. (°N)	Long. (°W)	X_e	Y_e				
0*	27°11.7'	91°12.2'	265.0	-65.6	115.0	22.0	100.0	956.3
6	27°43.4'	91°9.4'	269.0	-15.3	115.0	22.0	98.0	958.0
12	28°16.4'	91°9.4'	269.0	36.5	115.0	23.0	92.0	959.4
18	28°54.5'	91°19.5'	255.0	97.0	115.0	24.0	92.0	960.7
24	29°35.8'	91°23.0'	250.0	162.7	135.0	24.0	90.0	961.7
30	30°16.7'	91°0.8'	281.5	228.8	150.0	50.0	60.0	970.5
36	30°35.5'	90°5.8'	358.3	259.0	70.0	50.0	60.0	985.4
42	30°43.8'	88°58.4'	452.0	272.0	60.0	22.0	65.0	990.2

* Program Time of 0 hrs = 0000 GMT, 3 Oct 1964.

Table 3

Program SSURGE III Wind Data for Hurricane Betsy Surge Simulation

PHI = 30.0
THIT = 16.0
RHIT = 32.0
PINF = 1014.56

Program Time (hrs)	Track Location				Rotation (°)	Radius To Maximum Wind (n. mi.)	Stationary Storm Maximum Wind (Knots)	Central Pressure (mb)
	Lat. (°N)	Long. (°W)	X_e	Y_e				
0*	26°21.3'	86°45.5'	639.0	-145.9	75.0	23.5	90.0	951.0
6	27°8.3'	88°3.5'	529.0	-71.5	75.0	27.0	90.0	949.0
9	27°43.8'	88°34.6'	485.6	-15.7	75.0	28.5	94.0	944.0
12	28°20.4'	89°10'	436.0	42.2	75.0	30.0	96.0	941.0
15	28°56.4'	89°50.5'	379.3	99.5	75.0	32.0	96.0	941.0
18	29°35.5'	90°31.8'	321.5	161.8	215.0	32.0	88.0	948.0
21	30°4.2'	91°3.9'	276.3	208.0	245.0	45.0	75.0	955.0
24	30°38.1'	91°33.2'	235.5	262.5	220.0	65.0	60.0	965.0
27	31°11.6'	91°55.9'	203.3	315.9	230.0	105.0	40.0	975.0

* Program Time of 0 hrs = 1200 GMT, 9 Sept 1965.

Table 4

Program SSURGE III Wind Data for Hurricane Carmen Surge Simulation

PHI = 25.0
THIT = 24.0
RHIT = 20.0
PINF = 1014.56

| Program Time (hrs) | Track Location | | | | Rotation (°) | Radius To Maximum Wind (n. mi.) | Stationary Storm Maximum Wind (Knots) | Central Pressure (mb) |
	Lat. (°N)	Long. (°W)	X_e	Y_e				
0*	25°43.2'	90°13.0'	340.8	-207.6	115.0	17.0	90.0	950.0
6	26°52.5'	90°13.0'	340.8	-103.0	115.0	17.0	100.0	950.0
12	27°48.0'	90°24.1'	332.4	-8.8	115.0	17.0	100.0	944.0
18	28°41.6'	90°48.3'	298.6	76.0	115.0	17.0	110.0	937.0
24	29°24.0'	91°8.3'	256.8	144.0	115.0	20.0	90.0	960.0
30	30°0.0'	92°6.3'	189.3	201.3	115.0	24.0	70.0	982.0
36	30°24.0'	92°41.7'	140.0	240.0	115.0	30.0	45.0	993.0

* Program Time of 0 hrs = 1200 GMT, 7 Sept 1974.

Table 5

SSURGE III Finite Height Coast Boundary Data for the Louisiana Coast – Hurricanes Flossy, Hilda, Betsy and Carmen Surge Study

Coast H Grid Point I	Values of Coastal Barrier Length L_c (x 500 ft) at Various Barrier Elevations Z_b (ft REL MSL)													Entrance Channel Width W_c (ft)	Discharge Coeff Times Cross Sectional Area $C_b A_c$ (ft²)	Coastal Water Surface Area at MLW Representative of H(I, JM) A_T (ft² x 10⁶)	Flood Region Number	Storage Area A_b (ft² x 10⁹)	Elevation Z_b (ft REL MSL)
	0	1	2	3	4	5	6	7	8	9	10	11						
1-10	NO FLOODING CONSIDERED																		
11	102	102	102	102	0									3000	0	960.0			
12	103	103	103	98	0											720.0			
13	98	98	98													510.0	I	0.001	-5
14	0	90	90	90	0											990.0		11.208	0
15	90	90	90	90	0									51000	104000	1140.0		28.812	1
16	36	86	86	86	0											1030.0		33.777	>5
17	82	82	82	82												710.0			
18	76	76	76	76												350.0			
19	75	75	35	35												260.0			
20	66	66	0	0												280.0	II	0.001	-5
21	62	62	0	0												280.0		6.412	0
22	58	58	0	0												250.0		28.854	1
23	54	54	0	16	0	0								9000	7000	170.0		32.200	>5
24	32	32	16	47	0											110.0			
25	47	47	47	23	0											110.0			
26	23	23	23											10500	10000	130.0			
27	0	23			23	12	0									150.0			
28	23	37	37	37	37	30	15							8000	18000	150.0	III	0.001	-5
29	37	20	20	15		0									8000	120.0		11.096	0
30	20				23	17	17	13	9	4	4	0		3000	8000	90.0		23.474	1
31	0				37	17	17							18000	18000	80.0		26.702	>5
32	21	21			17	0								8000	8000	70.0			
33	20	20			20									8000	8000	80.0			
34	36	36	36	36	36	26	12									80.0			
35	37	37	37	37	37	33	8	4	0							80.0	IV	0.001	-5
36	36	36	36	36	36	30	0									90.0		1.673	0
37	36	36	36	37	37	30	10	4	0	0						90.0		23.557	1
38	37	37	37	38	38	37	33	20	4	0						100.0		28.715	>5
39	38	38	38	38	38	38	33	20								110.0			
40	42	42	42	42	42	30	15		0					2000	2000	130.0	V	0.001	-5
41	48	48	24	0	0									3000	7000	160.0		5.018	0
42	62	62	62	0	0									3000	1000	180.0		11.939	1
43	NO FLOODING CONSIDERED																	14.441	>5
44	80	80	80	0	0											250.0	VI	0.001	-8
45	90	90	90	0	0											310.0		12.127	-5
46	102	102	102	0	0											430.0		14.636	0
47	115	115	115	0	0											610.0		34.569	1
48	64	64	64	0	0									33000	49000	980.0		34.848	>5
49-52	NO FLOODING CONSIDERED																		

Table 6

Comparison of Computed and Observed Coastal

High Water Levels for Hurricane Flossy

Coastal Location	Computed* High Water Level (ft)	Observed High Water Level (ft)
6.1 n.mi. East of East Timbalier I. at Bay Champagne	2.3	3.7 (EST**)
Southwest Pass Ent.	2.0	3.7
Quarantine Bay	9.6	10.8, 11.9, 12.1
Pointe A La Hache, LA to Point Pleasant, LA	8.9	10.3, 10.5 (EST) 10.7, 11.0 (EST)
Breton I.	6.0	7 to 8 (EST)

* Adjusted for astronomical tide.
** Furnished by various oil companies and by the Freeport Sulphur Co.

Table 7

Comparison of Computed and Observed Inland

High Water Levels for Hurricane Flossy

Inland Location	Computed* High Water Level (ft)	Observed High Water Level (ft)
Barataria Bay to Mississippi River Levee, Flood Region 5	0.4	3.6**, 3.6**, 5.2**, 5.5**, 6.9**, 7.3**, 8.0**
Lake Borgne, Flood Region 6	2.5	4.0, 5.2, 6.3, 8.5, 6.2†, 6.4†, 6.9†, 7.7†, 8.1†, 8.6†, 9.4†, 10.9†

NOTE: Flood Regions 1 – 4 not affected.
  * Not adjusted for astronomical tide.
 ** Observations were located along landward side of coastal barrier.
  † Observations were located along southwest side of Lake Borgne.

Table 8

Comparison of Computed and Observed Coastal

High Water Levels for Hurricane Hilda

Coastal Location	Computed* High Water Level (ft)	Observed High Water Level (ft)
Gulf Ent., Freshwater Bayou	1.5	2.3
East Cote Blanche Bay at Lukes Landing, LA	2.5	4.4
Atchafalaya Bay at Eugene I.	3.8 (w/o flooding coast, 4.3)	3.3
Lake Pelto, 2.4 n.mi. Landward from Ent. to Terrebonne Bay	6.8 (w/o flooding coast, 7.2)	7.4
Grand I.	3.2 (w/o flooding coast, 3.2)	4.0
East Side Barataria Bay near Gulf Ent.	5.0	5.5
Southwest Pass, Mississippi River	1.5	3.2, 3.5
Quarantine Bay at Ostrica, LA	4.0 (w/o flooding coast, 4.4)	4.6
Ent. Mississippi River – Gulf Outlet Canal	4.0 (w/o flooding coast, 4.4)	4.6
Biloxi, MS	5.2 (w/o flooding coast, 5.2)	4.6

* Adjusted for astronomical tide.

Table 9

Comparison of Computed and Observed Inland

High Water Levels for Hurricane Hilda

Inland Location	Computed* High Water Level (ft)	Observed High Water Level (ft)
Atchafalaya Bay, Flood Region I	0.	3.8, 5.1
Atchafalaya River to Houma Canal, Flood Region II	3.8	None
Terrebonne-Timbalier Bay, Flood Region III	3.4	3.0, 3.8, 4.0, 4.7, 5.4, 6.6, 6.9, 6.9, 7.0, 7.4, 9.8
Bayou Lafourche to Barataria Bay, Flood Region IV	0.5	None
Barataria Bay to Mississippi River Levee, Flood Region V	1.6	4.0
Lake Borgne, Flood Region VI	3.3	3.8, 4.5, 4.7, 5.0, 5.2, 5.3

* Not adjusted for astronomical tide.

Table 10

Comparison of Computed and Observed Coastal
High Water Levels for Hurricane Betsy

Coastal Location	Computed* High Water Level (ft)	Observed High Water Level (ft)
East Cote Blanche Bay at Lukes Landing, LA	.4.5	3.8
Grand I.	7.2 (w/o flooding 7.4)	8.8
East Side Barataria Bay near Gulf Ent.	8.5 (w/o flooding coast, 9.8)	7.6
West Side Mississippi River Levee; Empire, LA, to Venice, LA	6.2 to 12.2 (w/o flooding coast, 6.2 to 16.1)	5.7, 7.4, 7.7, 8.8, 9.2, 10.4
East Side Mississippi River Levee; Pointe A La Hache, LA, to Ostrica (Brenton Sound), LA	12.4 to 15.2 (w/o flooding coast, 12.8 to 23.1)	13.6, 13.7, 14.4, 14.5, 15.7
Gulfport, MS	9.0 (Approx.)	10.7
Biloxi, MS	7.6	8.6

* Adjusted for astronomical tide.

Table 11

Comparison of Computed and Observed Inland
High Water Levels for Hurricane Betsy

Inland Location	Computed* High Water Level (ft)	Observed High Water Level (ft)
Atchafalaya Bay, Flood Region I	0.	2.9, 3.9
Atchafalaya River to Houma Canal, Flood Region II	0.9	3.0, 4.3 (along Houma Canal)
Terrebonne-Timbalier Bay, Flood Region III	1.8	2.8, 3.0, 4.3
Bayou Lafourche to Barataria Bay, Flood Region IV	0.5	3.4, 5.4
Barataria Bay to Mississippi River Levee, Flood Region V	2.1	3.4, 5.0, 5.3
Lake Borgne, Flood Region VI	7.1	6.4, 8.3, 8.8, 9.1, 9.3, 9.8, 10.1, 10.7, 11.0, 11.7, 14.4

* Not adjusted for astronomical tide.

Table 12

Comparison of Computed and Observed Coastal
High Water Levels for Hurricane Carmen

Coastal Location	Computed* High Water Level (ft)	Observed High Water Level (ft)
East Cote Blanche Bay at Lukes Landing, LA	4.3**	4.5
Atchafalaya Bay at Lower Atchafalaya River	4.5**	4.9
Atchafalaya Bay at Eugene I.	3.8 (w/o flooding coast, 4.0)	3.7
Grand I.	4.7 (w/o flooding coast, 4.8)	4.2
Ent. Mississippi River – Gulf Outlet Canal	5.1 (w/o flooding coast, 5.4)	5.7
Biloxi, MS	4.0 (w/o flooding coast, no change)	4.5
Caillou Bay	9.2 (w/o flooding coast, 11.6)	None
Ent. Terrebonne Bay	8.7 (w/o flooding coast, 11.1)	None

* Adjusted for astronomical tide.

** The time of high water occurred after 1200 CST 8 Sept 1974. The water level is approximate because the structure of the storm after 1200 CST is uncertain due to its rapid decay. Computations ended at 1800 CST 8 Sept.

Table 13

Comparison of Computed and Observed Inland
High Water Levels for Hurricane Carmen

Inland Location	Computed* High Water Level (ft)	Observed High Water Level (ft)
Atchafalaya Bay, Flood Region I	0.6**	2.8, 3.2, 3.8, 4.0, 4.8
Atchafalaya River to Houma Canal, Flood Region II	3.8	3.3
Terrebonne-Timbalier Bay, Flood Region III	4.4	2.9, 3.8, 4.6, 5.9, 11.6
Bayou Lafourche to Barataria Bay, Flood Region IV	0.5	None
Barataria Bay to Mississippi River Levee, Flood Region V	1.4	3.1
Lake Borgne, Flood Region VI	3.4	5.0, 6.0

* Not adjusted for astronomical tide.

** Computed bay level rising at end of computation. See footnote **, Table 18.
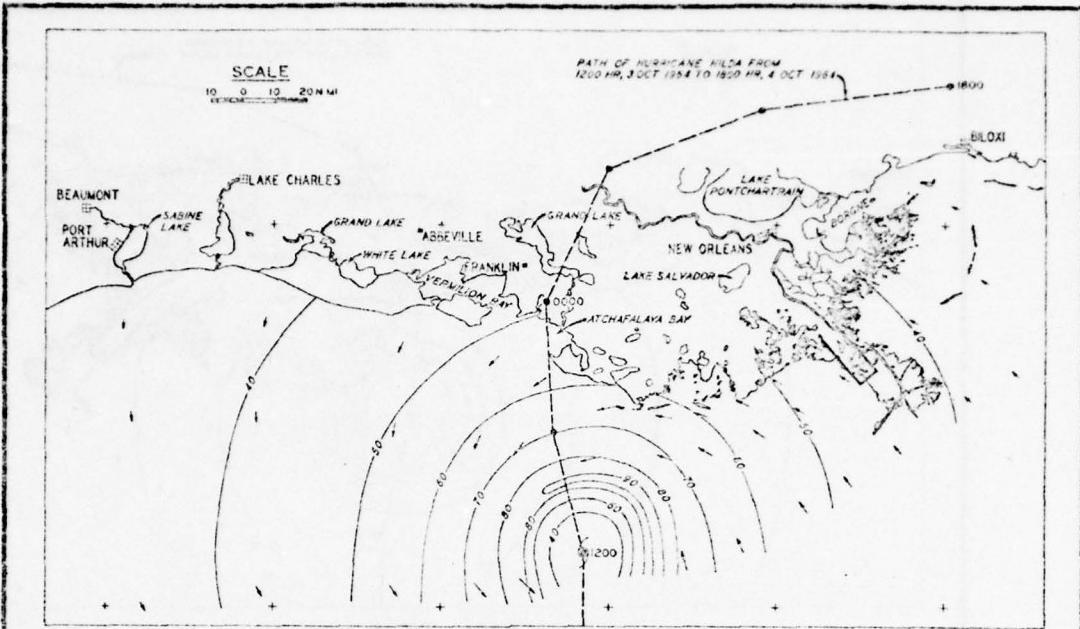
ANALYTICAL
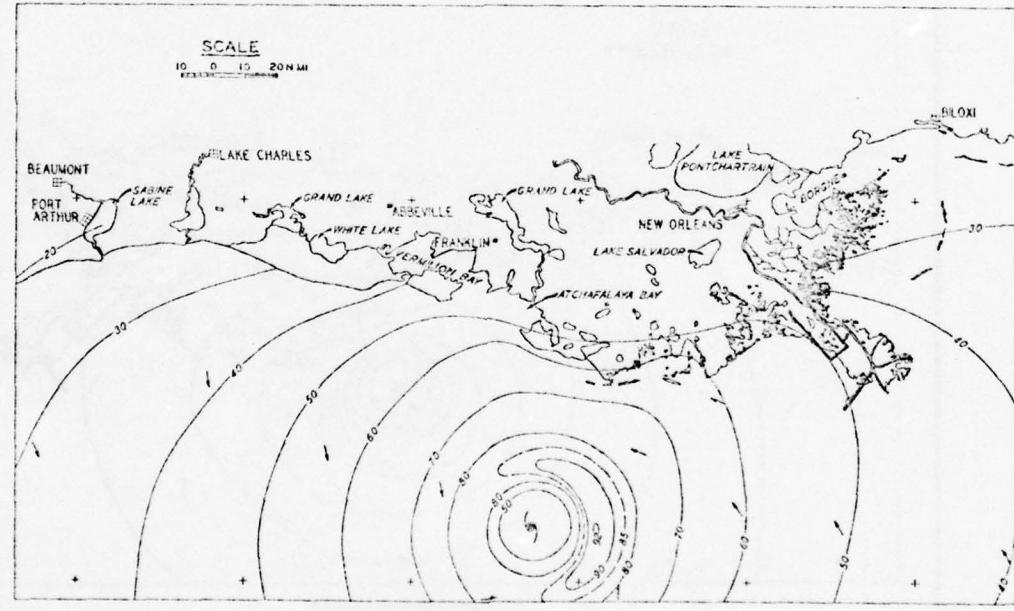
OBSERVED

LOUISIANA COAST SURGE STUDY

HURRICANE HILDA
ANALYTICAL AND OBSERVED
SURFACE WIND FIELD
AT 1200 HRS, 3 OCT 1964
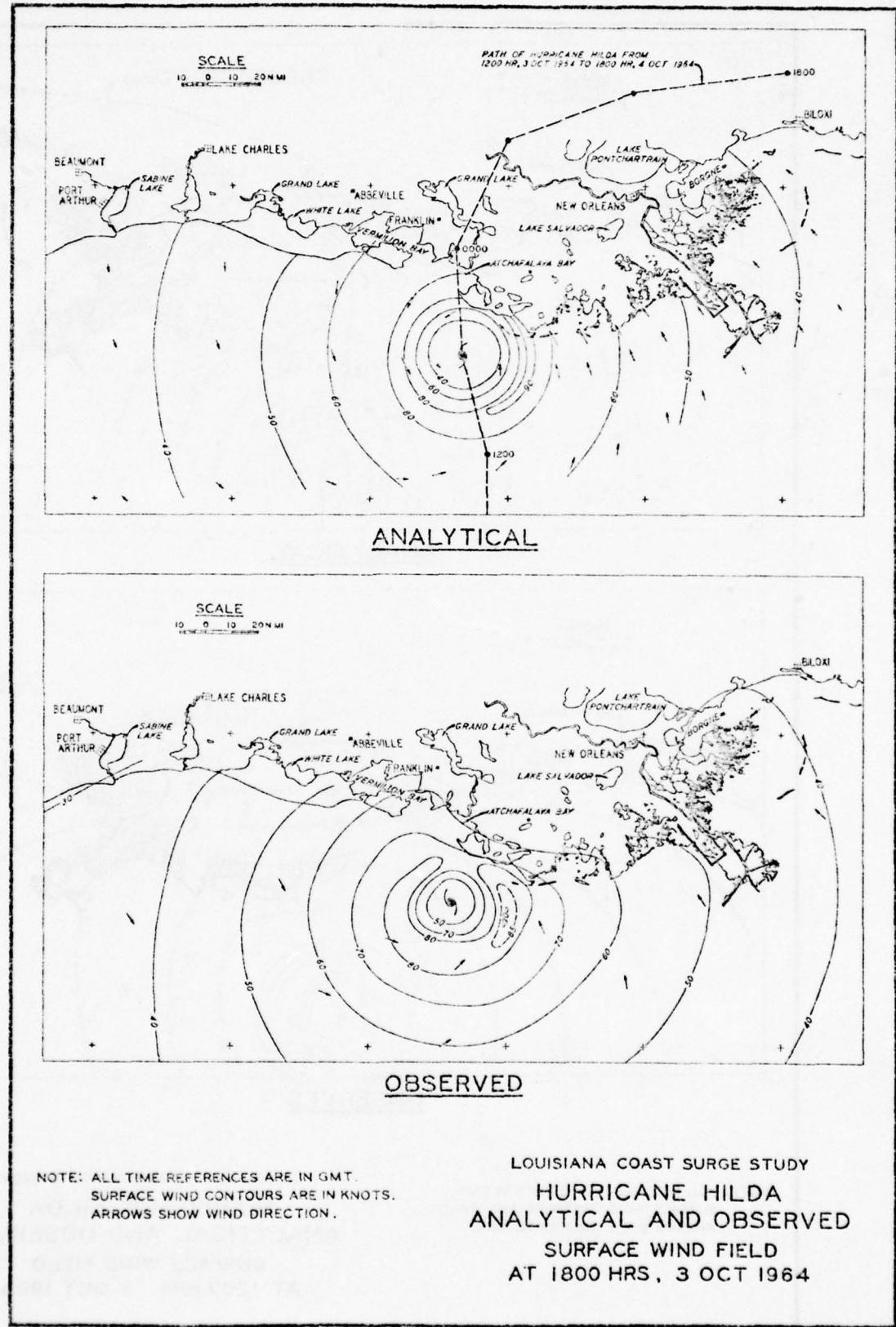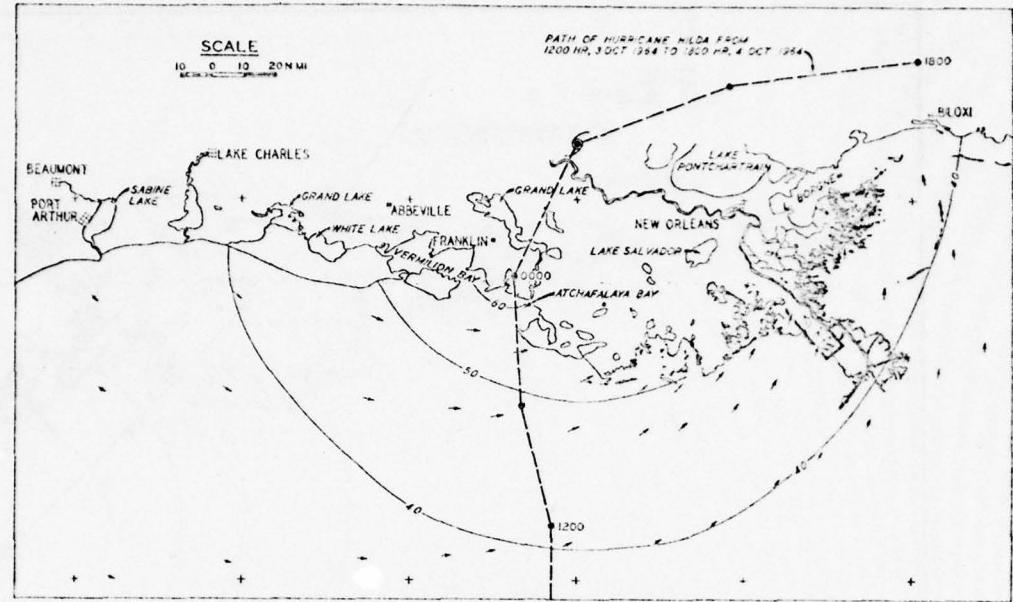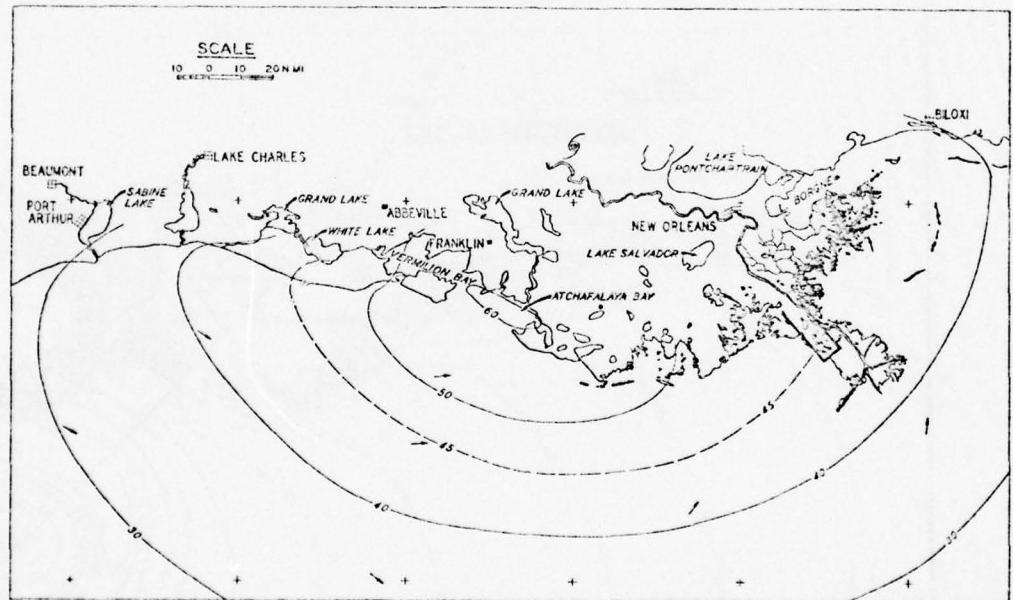
NOTE: ALL TIME REFERENCES ARE IN GMT.
SURFACE WIND CONTOURS ARE IN KNOTS.
ARROWS SHOW WIND DIRECTION.

PLATE 1

SCALE
10 0 10 20 N MI

PATH OF HURRICANE HILDA FROM
1200 HR, 3 OCT 1954 TO 1800 HR, 4 OCT 1964

ANALYTICAL

SCALE
10 0 10 20 N MI

OBSERVED

NOTE: ALL TIME REFERENCES ARE IN GMT.
SURFACE WIND CONTOURS ARE IN KNOTS.
ARROWS SHOW WIND DIRECTION.

LOUISIANA COAST SURGE STUDY
HURRICANE HILDA
ANALYTICAL AND OBSERVED
SURFACE WIND FIELD
AT 1800 HRS, 3 OCT 1964

PLATE 2

SCALE
10   0   10   20 N MI

PATH OF HURRICANE HILDA FROM
1200 HR, 3 OCT 1964 TO 1800 HR, 4 OCT 1964

ANALYTICAL

SCALE
10   0   10   20 N MI

OBSERVED

NOTE: ALL TIME REFERENCES ARE IN GMT.
SURFACE WIND CONTOURS ARE IN KNOTS.
ARROWS SHOW WIND DIRECTION.

LOUISIANA COAST SURGE STUDY
HURRICANE HILDA
ANALYTICAL AND OBSERVED
SURFACE WIND FIELD
AT 0600 HRS, 4 OCT 1964

PLATE 3
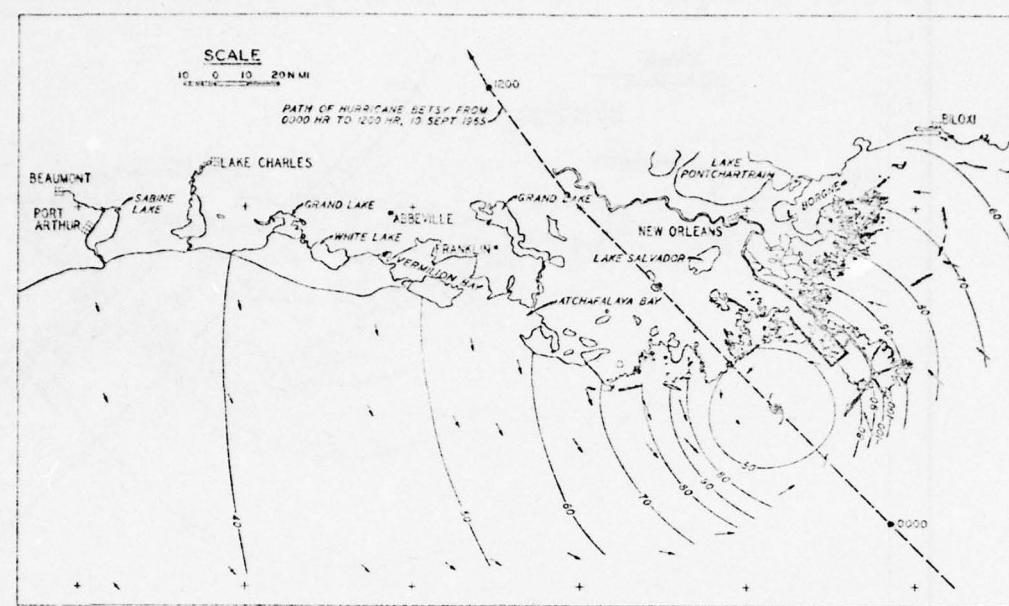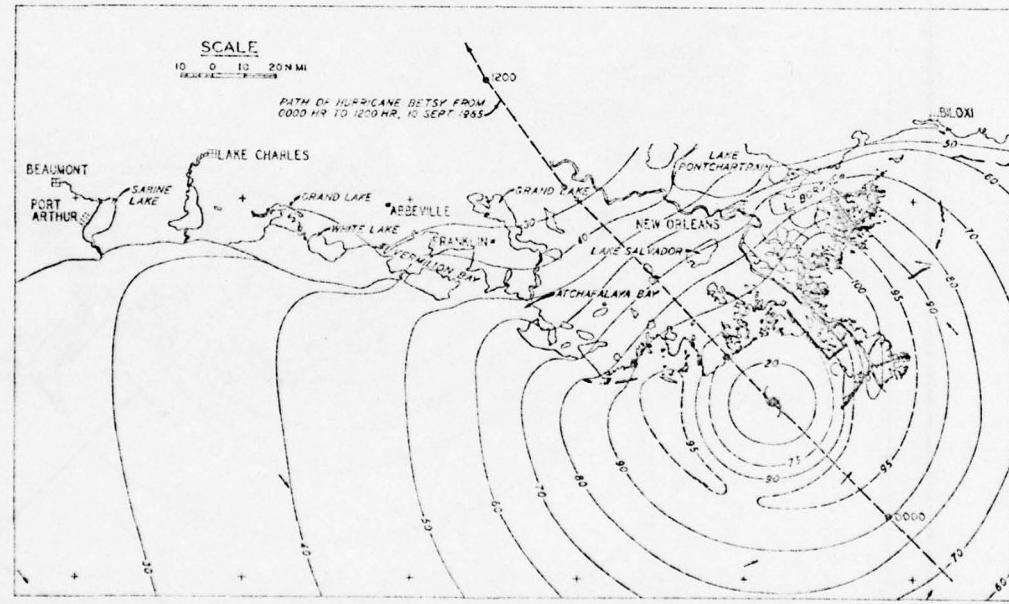
ANALYTICAL

OBSERVED

NOTE: ALL TIME REFERENCES ARE IN GMT.
SURFACE WIND CONTOURS ARE IN KNOTS.
ARROWS SHOW WIND DIRECTION.

LOUISIANA COAST SURGE STUDY
HURRICANE BETSY
ANALYTICAL AND OBSERVED
SURFACE WIND FIELD
AT 0000 HRS, 10 SEPT 1965

PLATE 4

ANALYTICAL

OBSERVED

NOTE: ALL TIME REFERENCES ARE IN GMT.
SURFACE WIND CONTOURS ARE IN KNOTS.
ARROWS SHOW WIND DIRECTION.

LOUISIANA COAST SURGE STUDY

HURRICANE BETSY
ANALYTICAL AND OBSERVED
SURFACE WIND FIELD
AT 0300 HRS, 10 SEPT 1965
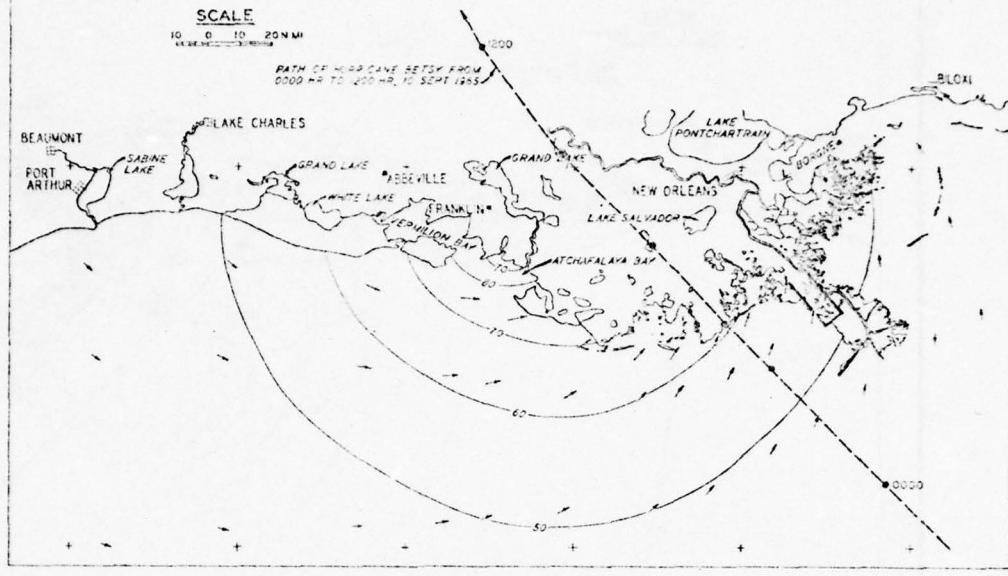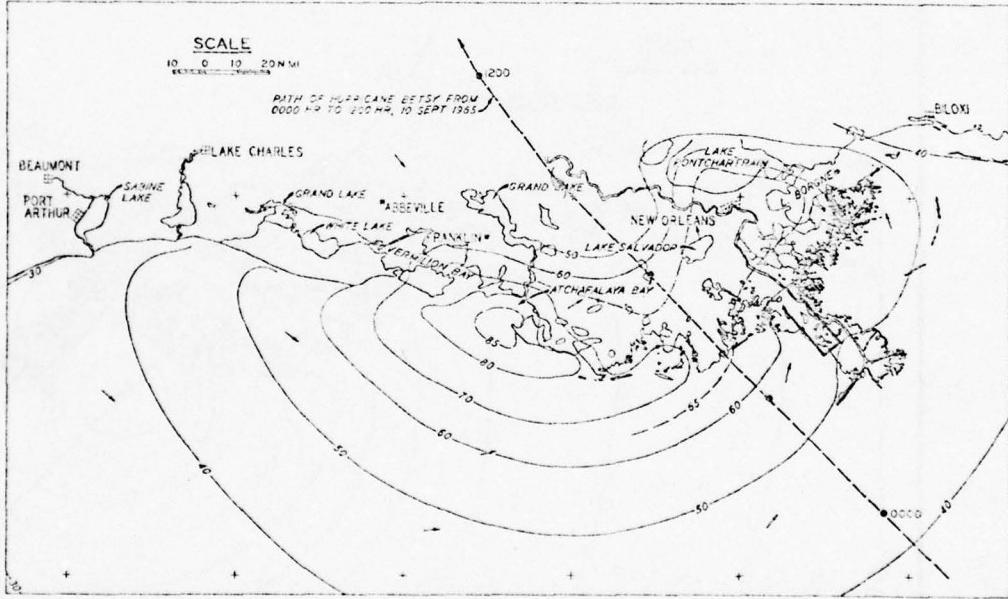
PLATE 5

ANALYTICAL

OBSERVED

NOTE: ALL TIME REFERENCES ARE IN GMT.
SURFACE WIND CONTOURS ARE IN KNOTS.
ARROWS SHOW WIND DIRECTION.

LOUISIANA COAST SURGE STUDY

HURRICANE BETSY
ANALYTICAL AND OBSERVED
SURFACE WIND FIELD
AT 0900 HRS, 10 SEPT 1965

PLATE 6

LOUISIANA COAST SURGE STUDY

LOCATION MAP AND
COMPUTING GRID

PLATE 7

SCALE

BILOXI

I=52

LAKE PONTCHARTRAIN

BORGNE

GRAND LAKE

ABBEVILLE

NEW ORLEANS

FRANKLIN

LAKE SALVADOR

VERMILION BAY

I=11

ATCHAFALAYA BAY

CAILLOU BAY

TERREBONNE BAY

TIMBALIER BAY

BARATARIA BAY

LOUISIANA COAST SURGE STUDY

**HURRICANE FLOSSY
SURGE SIMULATION**

STORM SURGE ENVELOPE

LEGEND

---- FLOOD COAST
—— WALL COAST

NOTE: COMPUTED SURGE NOT ADJUSTED
FOR ASTRONOMICAL TIDE

NOTE: ✱✱ HEAVY LINE REPRESENTS MISSISSIPPI
RIVER DELTA LEVEES, NUMERICALLY
SIMULATED BY TRANSPORT = 0.

PLATE 8

LEGEND

Inner limit of tidal overflow

Areas protected by levees and / or
seawalls which were overtopped and
inundated.

12.05   All elevations refer to mean sea level
datum Elevations shown are highest
reached by the hurricane tide. Elevations
were taken from all types of gages and
from high water marks. The elevations
noted as estimated were furnished by
various oil companies and by the Freeport
Sulphur Co.

MEMORANDUM REPORT
HURRICANE FLOSSY - SEPTEMBER, 1956
(WITHIN THE NEW ORLEANS DISTRICT)

AREA OF TIDAL OVERFLOW

SCALE OF MILES

U S ARMY ENGINEER DISTRICT NEW ORLEANS, LA
CORPS OF ENGINEERS

TO ACCOMPANY REPORT DATED   FILE NO

PLATE 9

LOUISIANA COAST SURGE STUDY

HURRICANE HILDA
SURGE SIMULATION

SURFACE TOPOGRAPHY CONTOUR
AND VELOCITY FOR WALL AND
FLOODING COAST BOUNDARY

1200 HOURS, 3 OCTOBER 1964

LEGEND

— 2 — WALL COAST } WATER SURFACE CONTOUR, FT
— 2 — FLOODING COAST }
— † WALL COAST } DEPTH AVERAGED VELOCITY
— † FLOODING COAST }

NOTE: ALL DEPTHS ARE IN FATHOMS.
KM HEAVY LINE REPRESENTS MISSISSIPPI
RIVER DELTA LEVEES, NUMERICALLY
SIMULATED BY TRANSPORT = 0.
ALL TIME REFERENCES ARE IN GMT.

PLATE 10

SCALE
10 0 10 20 MI

PATH OF HURRICANE HILDA FROM
1200 HR, 3 OCT 1964 TO 1800 HR, 4 OCT 1964

BEAUMONT
PORT ARTHUR
SABINE LAKE
LAKE CHARLES
GRAND LAKE
WHITE LAKE
ABBEVILLE
FRANKLIN
VERMILION BAY
GRAND LAKE
LAKE BORGNE
LAKE PONTCHARTRAIN
NEW ORLEANS
LAKE SALVADOR
ATCHAFALAYA BAY
BILOXI

SCALE
5   0   5
10 FPS

LEGEND

—2— WALL COAST ⎤
--2-- FLOODING COAST⎦ WATER SURFACE CONTOUR, FT
→ WALL COAST ⎤
⇢ FLOODING COAST⎦ DEPTH AVERAGED VELOCITY

NOTE: ALL DEPTHS ARE IN FATHOMS.
** HEAVY LINE REPRESENTS MISSISSIPPI
RIVER DELTA LEVEE NUMERICALLY
SIMULATED BY TRANSPORT= O.
ALL TIME REFERENCES ARE IN GMT.

LOUISIANA COAST SURGE STUDY

HURRICANE HILDA
SURGE SIMULATION

SURFACE TOPOGRAPHY CONTOUR
AND VELOCITY FOR WALL AND
FLOODING COAST BOUNDARY

1800 HOURS, 3 OCTOBER 1964

PLATE 11

PLATE 12

SCALE
10   0   10   20 N MI

PATH OF HURRICANE HILDA FROM
1200 HR, 3 OCT 1964 TO 1200 HR, 4 OCT 1964

1800

BILOXI

BEAUMONT
PORT ARTHUR
SABINE LAKE

LAKE CHARLES
GRAND LAKE

WHITE LAKE
ABBEVILLE
FRANKLIN
VERMILION BAY

GRAND LAKE

LAKE PONTCHARTRAIN

NEW ORLEANS

LAKE BORGNE

LAKE SALVADOR
ATCHAFALAYA BAY

0000

1200

SCALE
5   0   5   10 FPS

LEGEND

-- -2 --   WALL COAST
-- -2 --   FLOODING COAST] WATER SURFACE CONTOUR, FT
↑   WALL COAST
↑   FLOODING COAST] DEPTH AVERAGED VELOCITY

NOTE: ALL DEPTHS ARE IN FATHOMS.
XX HEAVY LINE REPRESENTS MISSISSIPPI
    RIVER DELTA LEVEES, NUMERICALLY
    SIMULATED BY TRANSPORT=0.
    ALL TIME REFERENCES ARE IN GMT.

LOUISIANA COAST SURGE STUDY
HURRICANE HILDA
SURGE SIMULATION

SURFACE TOPOGRAPHY CONTOUR
AND VELOCITY FOR WALL AND
FLOODING COAST BOUNDARY

0000 HOURS, 4 OCTOBER 1964

LOUISIANA COAST SURGE STUDY

HURRICANE HILDA
SURGE SIMULATION

SURFACE TOPOGRAPHY CONTOUR
AND VELOCITY FOR WALL AND
FLOODING COAST BOUNDARY

0600 HOURS, 4 OCTOBER 1964

PATH OF HURRICANE HILDA FROM
1200 HR 3 OCT 1954 TO 1800 HR 4 OCT 1954

1800

BILOXI

1000

LAKE PONTCHARTRAIN

BORGNE

NEW ORLEANS

LAKE SALVADOR

GRAND LAKE

ATCHAFALAYA BAY

FRANKLIN

ABBEVILLE

WHITE LAKE

VERMILION BAY

GRAND LAKE

LAKE CHARLES

BEAUMONT

PORT ARTHUR

SABINE LAKE

1200

0

0

0

0

0

-10

-10

-50

-50

-50

SCALE

10   0   10   20 N MI

SCALE

5   0   5   10 FPS

LEGEND

—2— WALL COAST } WATER SURFACE CONTOUR, FT
—2— FLOODING COAST

→ WALL COAST } DEPTH AVERAGED VELOCITY
→ FLOODING COAST

NOTE: ALL DEPTHS ARE IN FATHOMS.
HEAVY LINE REPRESENTS MISSISSIPPI
RIVER DELTA LEVEES, NUMERICALLY
SIMULATED BY TRANSPORT = 0
ALL TIME REFERENCES ARE IN GMT.

PLATE 13

LOUISIANA COAST SURGE STUDY

HURRICANE HILDA
SURGE SIMULATION

SURFACE TOPOGRAPHY CONTOUR
AND VELOCITY FOR WALL AND
FLOODING COAST BOUNDARY

1200 HOURS, 4 OCTOBER 1964

LEGEND

—2—— WALL COAST } WATER SURFACE CONTOUR, FT
——2—— FLOODING COAST
——→ WALL COAST } DEPTH AVERAGED VELOCITY
——→ FLOODING COAST

NOTE: ALL DEPTHS ARE IN FATHOMS.
HEAVY LINE REPRESENTS MISSISSIPPI
RIVER DELTA LEVELS, NUMERICALLY
SIMULATED BY TRANSPORT=0.
ALL TIME REFERENCES ARE IN GMT.

PLATE 14

HURRICANE HILDA
SURGE SIMULATION

SURFACE TOPOGRAPHY CONTOUR AND VELOCITY FOR WALL AND FLOODING COAST BOUNDARY
1300 HOURS, 4 OCTOBER 1964

BILOXI

PATH OF HURRICANE HILDA FROM 1200 HR, 3 OCT 1964 TO 1800 HR, 4 OCT 1964

LAKE PONTCHARTRAIN

BORGNE

NEW ORLEANS

LAKE SALVADOR

ATCHAFALAYA BAY

GRAND LAKE

FRANKLIN

ABBEVILLE

WHITE LAKE

VERMILION BAY

COCO

GRAND LAKE

LAKE CHARLES

SABINE LAKE

BEAUMONT

PORT ARTHUR

SCALE
10 0 10 20 NM

SCALE
0 5

5 0 5 10 FPS

LEGEND

—2— WALL COAST
— 2 — FLOODING COAST } WATER SURFACE CONTOUR, FT
→ WALL COAST
⇢ FLOODING COAST } DEPTH AVERAGED VELOCITY

NOTE: ALL DEPTHS ARE IN FATHOMS.
HEAVY LINE REPRESENTS MISSISSIPPI
RIVER DELTA LEVEES, NUMERICALLY
SIMULATED BY TRANSPORT=0.
ALL TIME REFERENCES ARE IN GMT.

PLATE 15

SCALE
10 0 10 20 N MI.

BILOXI

LAKE PONTCHARTRAIN

BORGNE

GRAND LAKE

ABBEVILLE

FRANKLIN

NEW ORLEANS

VERMILION BAY

LAKE SALVADOR

ATCHAFALAYA BAY

I = 11

CAILLOU BAY

TERREBONNE BAY

TIMBALIER BAY

BARATARIA BAY

I = 52

LEGEND
OBSERVED HIGH WATER ELEVATIONS
TIDE GAGE
STILL HIGH WATER MARK

DISTANCE ALONG MISSISSIPPI R. DELTA, A-D, N.MI.

WATER ELEVATION, FT REL MSL

LEGEND
--- FLOOD COAST
— WALL COAST
NOTE: COMPUTED SURGE NOT ADJUSTED FOR ASTRONOMICAL TIDE

SURGE ELEVATION, FT REL MSL

I = 11

MISS. R. DELTA LEVEES

I = 43

I = 52

DISTANCE ALONG COAST, N. MI.

NOTE: ✹✹ HEAVY LINE REPRESENTS MISSISSIPPI RIVER DELTA LEVEES, NUMERICALLY SIMULATED BY TRANSPORT = 0.

LOUISIANA COAST SURGE STUDY

HURRICANE HILDA
SURGE SIMULATION
STORM SURGE ENVELOPE

PLATE 16

WATER ELEVATION, FT REL MSL

OBSERVED

COMPUTED

TIME, HR

NOTE: PROGRAM TIME OF 0 HRS = 2400 GMT, 2 OCT 1964

LOUISIANA COAST SURGE STUDY

HURRICANE HILDA
SURGE SIMULATION

HYDROGRAPH
ATCHAFALAYA BAY
EUGENE ISLAND, LOUISIANA

PLATE 17

LOUISIANA COAST SURGE STUDY
HURRICANE HILDA
SURGE SIMULATION
HYDROGRAPH
QUARANTINE BAY
OSTRICA, LOUISIANA

NOTE: PROGRAM TIME OF 0 HRS = 2400 GMT, 2 OCT 1964

PLATE 18

LOUISIANA COAST SURGE STUDY
HURRICANE HILDA
SURGE SIMULATION
HYDROGRAPH
BILOXI, MISSISSIPPI

NOTE: PROGRAM TIME OF 0 HRS = 2400 GMT, 2 OCT 1964

PLATE 19

LOUISIANA COAST SURGE STUDY
HURRICANE HILDA
SURGE SIMULATION
HYDROGRAPH
ENTRANCE OF MISSISSIPPI RIVER
GULF OUTLET CANAL

NOTE: OBSERVED GAGE HIGH WATER = 4.6 FT.

NOTE: PROGRAM TIME OF 0 HRS = 2400 GMT, 2 OCT 1964

PLATE 20

LEGEND

◇ River Gage reading, including stream gage

Ⓣ Tide Gage reading

Ⓢ Still high water elevation

⌐ Existing levees

✕ Indicate elevation where not previously surveyed. Elevations are in feet and refer to Mean Sea Level.

HURRICANE HILDA 3-5 OCT 1964

AREA OF INUNDATION
AND HIGH WATER
ELEVATIONS

U.S. ARMY ENGINEER DISTRICT, NEW ORLEANS, LA.
TO ACCOMPANY REPORT ON HURRICANE
HILDA DATED MAY 1965 FILE No. H-2-23748

SCALE IN MILES

PLATE 21

PLATE 22

SCALE
10 0   10   20 N.MI

BILOXI

PATH OF HURRICANE BETSY FROM 0000 HR TO 1200 HR, 10 SEPT 1965

LAKE PONTCHARTRAIN

LAKE BORGNE

1200

NEW ORLEANS

GRAND LAKE

LAKE SALVADOR

ATCHAFALAYA BAY

0000

LAKE CHARLES

GRAND LAKE

WHITE LAKE

ABBEVILLE

FRANKLIN

VERMILION BAY

SABINE LAKE

BEAUMONT

PORT ARTHUR

50

SCALE

5   0   5
10 FPS

LOUISIANA COAST SURGE STUDY

HURRICANE BETSY
SURGE SIMULATION

SURFACE TOPOGRAPHY CONTOUR
AND VELOCITY FOR WALL AND
FLOODING COAST BOUNDARY

0000 HOURS, 10 SEPTEMBER 1965

LEGEND

2 —— WALL COAST
2 ---- FLOODING COAST } WATER SURFACE CONTOUR, FT
—→ WALL COAST
--→ FLOODING COAST } DEPTH AVERAGED VELOCITY

NOTE: ALL DEPTHS ARE IN FATHOMS.
XX HEAVY LINE REPRESENTS MISSISSIPPI
RIVER DELTA LEVEES, NUMERICALLY
SIMULATED BY TRANSPORT= 0.
ALL TIME REFERENCES ARE IN GMT.

LOUISIANA COAST SURGE STUDY
HURRICANE BETSY
SURGE SIMULATION
SURFACE TOPOGRAPHY CONTOUR
AND VELOCITY FOR WALL AND
FLOODING COAST BOUNDARY
0300 HOURS, 10 SEPTEMBER 1965

PLATE 23

LOUISIANA COAST SURGE STUDY

HURRICANE BETSY
SURGE SIMULATION

SURFACE TOPOGRAPHY CONTOUR
AND VELOCITY FOR WALL AND
FLOODING COAST BOUNDARY

0600 HOURS, 10 SEPTEMBER 1965

SCALE
10   0   10   20 N MI

SCALE
5   0   5
10 FPS

PATH OF HURRICANE BETSY FROM
0000 HR TO 1200 HR, 10 SEPT 1965

1200

0000

BILOXI

LAKE BORGNE

LAKE PONTCHARTRAIN

NEW ORLEANS

LAKE SALVADOR

GRAND LAKE

ATCHAFALAYA BAY

FRANKLIN

ABBEVILLE

WHITE LAKE

VERMILION BAY

GRAND LAKE

LAKE CHARLES

SABINE LAKE

BEAUMONT

PORT ARTHUR

LEGEND

WALL COAST
FLOODING COAST } WATER SURFACE CONTOUR, FT
WALL COAST
FLOODING COAST } DEPTH AVERAGED VELOCITY

NOTE: ALL DEPTHS ARE IN FATHOMS.
XX HEAVY LINE REPRESENTS MISSISSIPPI
RIVER DELTA LEVEES, NUMERICALLY
SIMULATED BY TRANSPORT = 0.
ALL TIME REFERENCES ARE IN GMT.

SCALE
10 0 10 20 N.MI.

BEAUMONT
PORT ARTHUR
SABINE LAKE

LAKE CHARLES

GRAND LAKE
GRAND LAKE
WHITE LAKE
ABBEVILLE
FRANKLIN
VERMILION BAY

200

PATH OF HURRICANE BETSY FROM
0000 HR TO 1200 HR, 10 SEPT 1965

LAKE
PONTCHARTRAIN

NEW ORLEANS

LAKE SALVADOR

ATCHAFALAYA BAY

BILOXI

10000

50

50

50

10

2

0

0

50

SCALE

5   0   5

10 FPS

LEGEND

WALL COAST
FLOODING COAST } WATER SURFACE CONTOUR, FT

WALL COAST
FLOODING COAST } DEPTH AVERAGED VELOCITY

NOTE: ALL DEPTHS ARE IN FATHOMS
AN HEAVY LINE REPRESENTS MISSISSIPPI
RIVER DELTA LEVEES. NUMERICALLY
SIMULATED BY TRANSPORT = 0
ALL TIME REFERENCES ARE IN GMT

LOUISIANA COAST SURGE STUDY

HURRICANE BETSY
SURGE SIMULATION

SURFACE TOPOGRAPHY CONTOUR
AND VELOCITY FOR WALL AND
FLOODING COAST BOUNDARY

0900 HOURS, 10 SEPTEMBER 1965

LOUISIANA COAST SURGE STUDY

HURRICANE BETSY
SURGE SIMULATION

SURFACE TOPOGRAPHY CONTOUR
AND VELOCITY FOR WALL AND
FLOODING COAST BOUNDARY

1500 HOURS, 10 SEPTEMBER 1965

SCALE

SCALE

10 FPS

LEGEND

—2— WALL COAST } WATER SURFACE CONTOUR, FT
--2-- FLOODING COAST
→ WALL COAST } DEPTH AVERAGED VELOCITY
→ FLOODING COAST

NOTE: ALL DEPTHS ARE IN FATHOMS.
HEAVY LINE REPRESENTS MISSISSIPPI
RIVER DELTA LEVEES, NUMERICALLY
SIMULATED BY TRANSPORT=O
ALL TIME REFERENCES ARE IN CMT.

PATH OF HURRICANE BETSY FROM
0000 HR TO 1200 HR, 10 SEPT 1965

TO 1500
1200
0000

BILOXI
LAKE PONTCHARTRAIN
BORGNE
NEW ORLEANS
LAKE SALVADOR
ATCHAFALAYA BAY
GRAND LAKE
FRANKLIN
VERMILION BAY
ABBEVILLE
WHITE LAKE
GRAND LAKE
LAKE CHARLES
SABINE LAKE
BEAUMONT
PORT ARTHUR

PLATE 27

SCALE

10 0 10 20 N.MI

BILOXI

LAKE PONTCHARTRAIN

GRAND LAKE

BORGNE

ABBEVILLE

NEW ORLEANS

FRANKLIN

LAKE SALVADOR

VERMILION BAY

I = 52

I = 11

ATCHAFALAYA BAY

LEGEND

OBSERVED HIGH WATER ELEVATIONS

○ TIDE GAGE

⬡ STILL HIGH WATER MARK

CAILLOU BAY

D

A

B

BARATARIA BAY

TERREBONNE BAY

TIMBALIER BAY

WATER ELEVATION, FT REL MSL

21

18

15

12

9

6

3

A B C D

0 20 40 60

DISTANCE ALONG MISSISSIPPI R.
DELTA, A-D, N.MI.

LEGEND

----- FLOOD COAST

——— WALL COAST

NOTE: COMPUTED SURGE NOT ADJUSTED
FOR ASTRONOMICAL TIDE

SURGE ELEVATION, FT REL MSL

24

21

18

15

12

9

6

3

0

I = 11

MR. DELTA LEVEES

XX

I = 43

I = 52

100 120 140 160 180 200 220 240 260 280 300 320 340 360 380

DISTANCE ALONG COAST, N.MI.

NOTE: XX HEAVY LINE REPRESENTS MISSISSIPPI
RIVER DELTA LEVEES, NUMERICALLY
SIMULATED BY TRANSPORT = 0.

LOUISIANA COAST SURGE STUDY

HURRICANE BETSY
SURGE SIMULATION
STORM SURGE ENVELOPE

LOUISIANA COAST SURGE STUDY
HURRICANE BETSY
SURGE SIMULATION
HYDROGRAPH
EAST COTE BLANCHE BAY
LUKE'S LANDING, LOUISIANA

NOTE: PROGRAM TIME OF 0 HRS = 1200 GMT, 9 SEPT 1965

PLATE 28

LOUISIANA COAST SURGE STUDY
HURRICANE BETSY
SURGE SIMULATION
HYDROGRAPH
BILOXI, MISSISSIPPI

NOTE: PROGRAM TIME OF 0 HRS = 1200 GMT, 9 SEPT 1965

PLATE 29

LEGEND

River Gage reading, including
stream gage
Tide Gage reading
Still high water elevation
Existing levees

Plates G thru II, details of
inundated area

Elevations are in feet and refer
to Mean Sea Level

HURRICANE BETSY 9-11 SEPT 1965

AREA OF INUNDATION
AND HIGH WATER
ELEVATIONS

U.S. ARMY ENGINEER DISTRICT, NEW ORLEANS, LA.
TO ACCOMPANY REPORT ON HURRICANE
BETSY DATED NOVEMBER 1965
FILE NO H-2-23645

PLATE 30

PLATE 31

SCALE
10   0   10   20 N MI

PATH OF HURRICANE CARMEN FROM
0600 HR TO 2400 HR, 8 SEPT 1974

2400

2100

BEAUMONT
PORT ARTHUR
SABINE LAKE
LAKE CHARLES
GRAND LAKE
WHITE LAKE
ABBEVILLE
VERMILION BAY
FRANKLIN
GRAND LAKE
ATCHAFALAYA BAY
LAKE SALVADOR
NEW ORLEANS
LAKE PONTCHARTRAIN
BORGNE
BILOXI

0600 HRS

SCALE
5   0   5   10 FPS

LOUISIANA COAST SURGE STUDY

HURRICANE CARMEN
SURGE SIMULATION

SURFACE TOPOGRAPHY CONTOUR
AND VELOCITY FOR WALL AND
FLOODING COAST BOUNDARY
0600 HOURS, 8 SEPTEMBER 1974

LEGEND

—2— WALL COAST
—2— FLOODING COAST } WATER SURFACE CONTOUR, FT

——→ WALL COAST
——→ FLOODING COAST } DEPTH AVERAGED VELOCITY

NOTE: ALL DEPTHS ARE IN FATHOMS.
HEAVY LINE REPRESENTS MISSISSIPPI
RIVER DELTA LEVEES, NUMERICALLY
SIMULATED BY TRANSPORT = 0
ALL TIME REFERENCES ARE IN GMT.

PLATE 32

LOUISIANA COAST SURGE STUDY

HURRICANE CARMEN
SURGE SIMULATION

SURFACE TOPOGRAPHY CONTOUR
AND VELOCITY FOR WALL AND
FLOODING COAST BOUNDARY

1200 HOURS, 8 SEPTEMBER 1974

SCALE

10 0 10 20 N MI

SCALE

5 0 5 10 FPS

LEGEND

—2— WALL COAST
--2-- FLOODING COAST } WATER SURFACE CONTOUR, FT
WALL COAST
FLOODING COAST } DEPTH AVERAGED VELOCITY

NOTE: ALL DEPTHS ARE IN FATHOMS.
※※ HEAVY LINE REPRESENTS MISSISSIPPI
RIVER DELTA LEVEES, NUMERICALLY
SIMULATED BY TRANSPORT = 0.
ALL TIME REFERENCES ARE IN GMT.

PATH OF HURRICANE CARMEN FROM
0600 HR TO 2400 HR, 8 SEPT 1974

2400

BILOXI

LAKE PONTCHARTRAIN

LAKE BORGNE

NEW ORLEANS

LAKE SALVADOR

GRAND LAKE

ATCHAFALAYA BAY

FRANKLIN

ABBEVILLE

WHITE LAKE

GRAND LAKE

VERMILLION BAY

LAKE CHARLES

SABINE LAKE

BEAUMONT

PORT ARTHUR

50

50

10

0

SCALE

10   0   10   20 N MI

PATH OF HURRICANE CARMEN FROM
0600 HR TO 2400 HR, 8 SEPT 1974

2400

BILOXI

LAKE
PONTCHARTRAIN

BORGNE

LAKE

GRAND LAKE

NEW ORLEANS

LAKE SALVADOR

ATCHAFALAYA BAY

0600

FRANKLIN

VERMILION BAY

GRAND LAKE

ABBEVILLE

WHITE LAKE

BEAUMONT

PORT
ARTHUR

SABINE
LAKE

LAKE
CHARLES

SCALE

5   0   5   10 FMS

LEGEND

—2— WALL COAST
—2— FLOODING COAST } WATER SURFACE CONTOUR, FT
      WALL COAST
      FLOODING COAST } DEPTH AVERAGED VELOCITY

NOTE: ALL DEPTHS ARE IN FATHOMS
      HEAVY LINE REPRESENTS MISSISSIPPI
      RIVER DELTA LEVEES, NEVER ACTUALLY
   SIMULATED BY TRANSPORT=0
      ALL TIME REFERENCES ARE IN GMT.

LOUISIANA COAST SURGE STUDY

HURRICANE CARMEN
SURGE SIMULATION

SURFACE TOPOGRAPHY CONTOUR
AND VELOCITY FOR WALL AND
FLOODING COAST BOUNDARY

1800 HOURS, 8 SEPTEMBER 1974

PLATE 33

SCALE

10   0   10   20 N MI

BILOXI

I=52

LAKE PONTCHARTRAIN

GRAND LAKE

BORGNE

ABBEVILLE

NEW ORLEANS

FRANKLIN

LAKE SALVADOR

VERMILION BAY

D

LEGEND

OBSERVED HIGH WATER ELEVATIONS

I=11

TIDE GAGE

STILL HIGH WATER MARK

ATCHAFALAYA BAY

C

CAILLOU BAY

A

B

TERREBONNE BAY

TIMBALIER BAY

BARATARIA BAY

WATER ELEVATION, FT REL MSL

8

6

4

2

0

A   B   C   D

0   20   40   60

DISTANCE ALONG MISSISSIPPI R
DELTA, A-D, N MI

LEGEND

– – – FLOOD COAST
———— WALL COAST

NOTE: COMPUTED SURGE NOT ADJUSTED
FOR ASTRONOMICAL TIDE

SURGE ELEVATION, FT REL MSL

12

10

8

6

4

2

0

MISS. R. DELTA LEVEES

I=11

I=43

**

I=52

100 120 140 160 180 200 220 240 260 280 300 320 340 360 380

DISTANCE ALONG COAST, N MI

NOTE: ✱✱ HEAVY LINE REPRESENTS MISSISSIPPI
RIVER DELTA LEVEES, NUMERICALLY
SIMULATED BY TRANSPORT = 0

LOUISIANA COAST SURGE STUDY

HURRICANE CARMEN
SURGE SIMULATION
STORM SURGE ENVELOPE

PLATE 34

LOUISIANA COAST SURGE STUDY
HURRICANE CARMEN
SURGE SIMULATION
HYDROGRAPH
EAST COTE BLANCHE BAY
LUKE'S LANDING, LOUISIANA

NOTE: PROGRAM TIME OF 0 HRS = 1200 GMT, 7 SEPT 1974

PLATE 35

LOUISIANA COAST SURGE STUDY
HURRICANE CARMEN
SURGE SIMULATION
HYDROGRAPH
ATCHAFALAYA BAY AT
EUGENE ISLAND, LOUISIANA
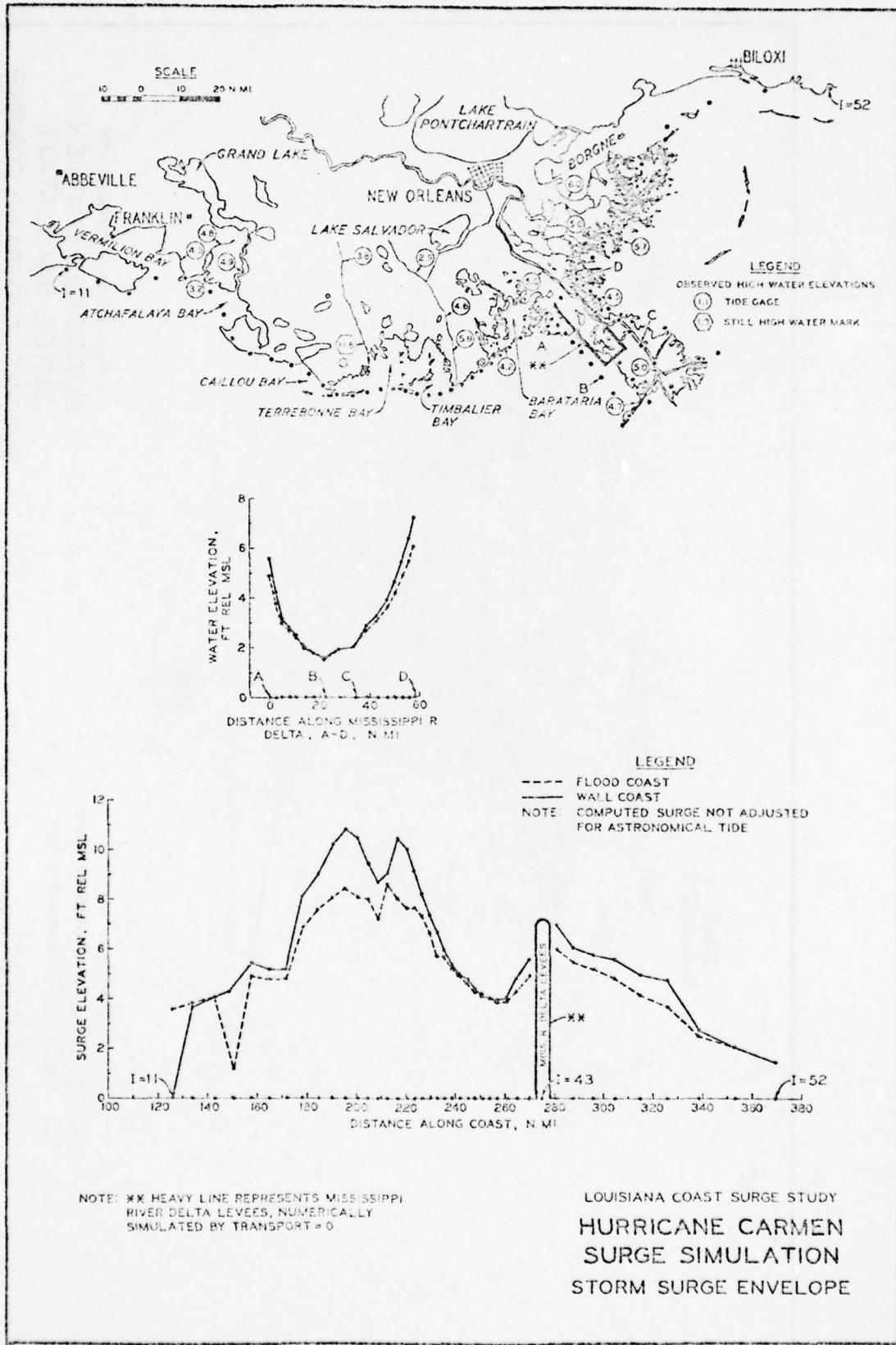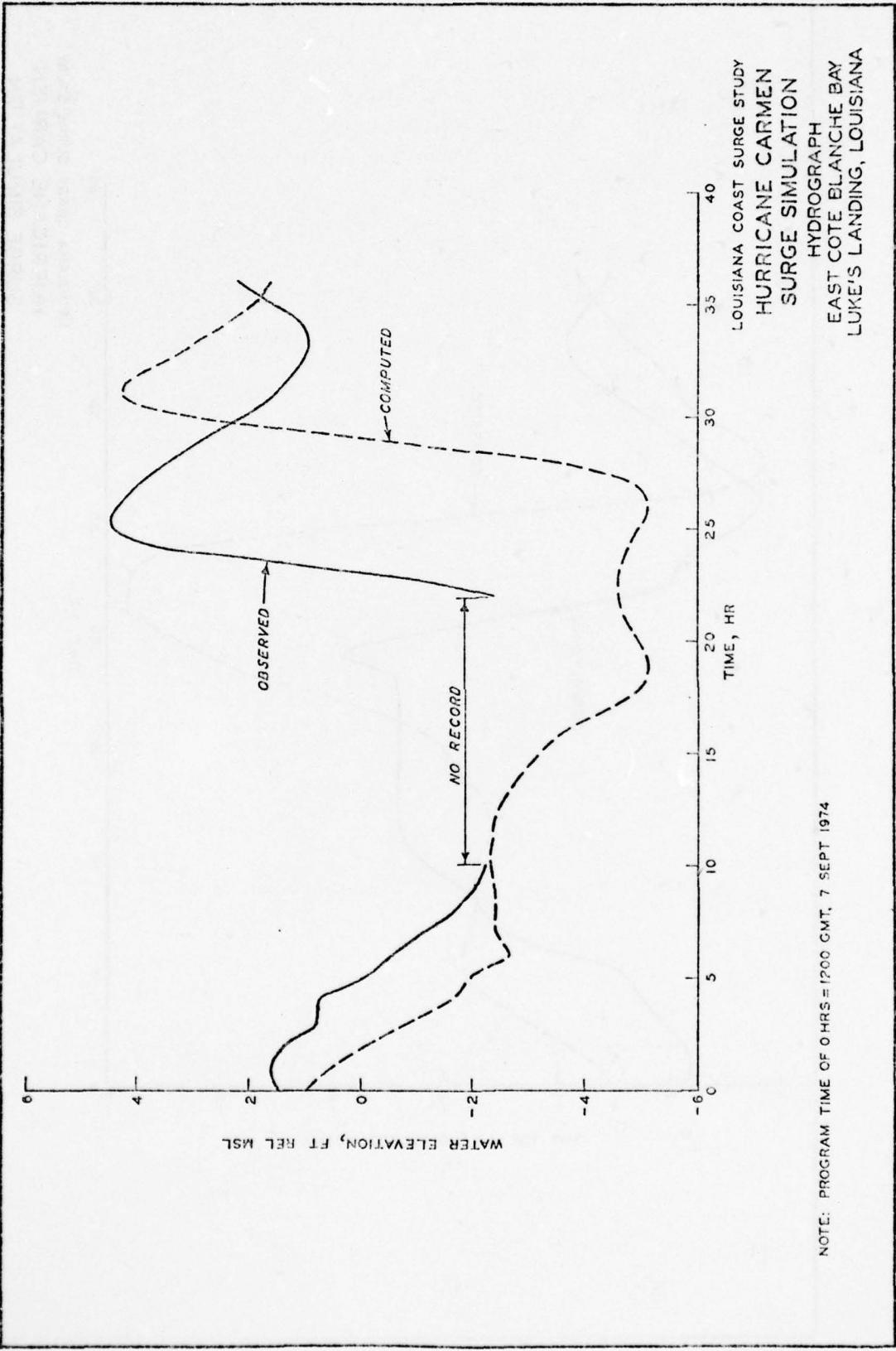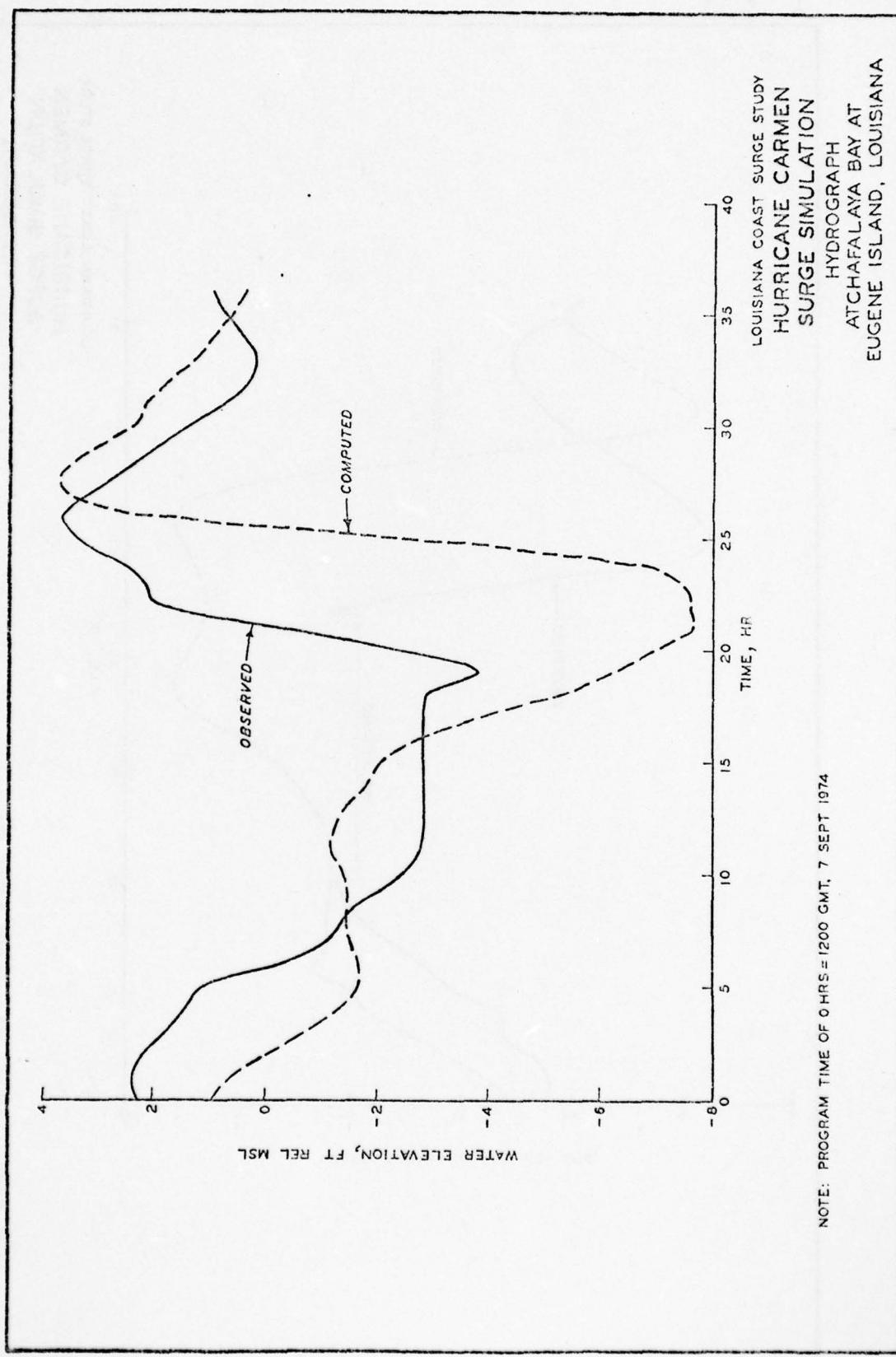
NOTE: PROGRAM TIME OF 0 HRS = 1200 GMT, 7 SEPT 1974

PLATE 36

LOUISIANA COAST SURGE STUDY
HURRICANE CARMEN
SURGE SIMULATION
HYDROGRAPH
GARDNER ISLAND, LOUISIANA
ENTRANCE OF MISSISSIPPI RIVER
GULF OUTLET CANAL

NOTE: PROGRAM TIME OF 0 HRS = 1200 GMT, 7 SEPT 1974

PLATE 37

LOUISIANA COAST SURGE STUDY
HURRICANE CARMEN
SURGE SIMULATION
HYDROGRAPH
BILOXI, MISSISSIPPI

NOTE: PROGRAM TIME OF 0 HRS = 1200 GMT, 7 SEPT 1974

PLATE 38

LEGEND

FLOOD ELEVATION DATA

Gage reading

Still high water mark

Levee

AREA FLOODED

HURRICANE CAMILLE 7-18 SEP 1974

U.S. ARMY ENGINEER DISTRICT, NEW ORLEANS
CORPS OF ENGINEERS

DEC 1974   FILE NO. H-2-27080

SCALE OF MILES

GULF OF MEXICO

ALA.
MISS.

MISSISSIPPI
LOUISIANA
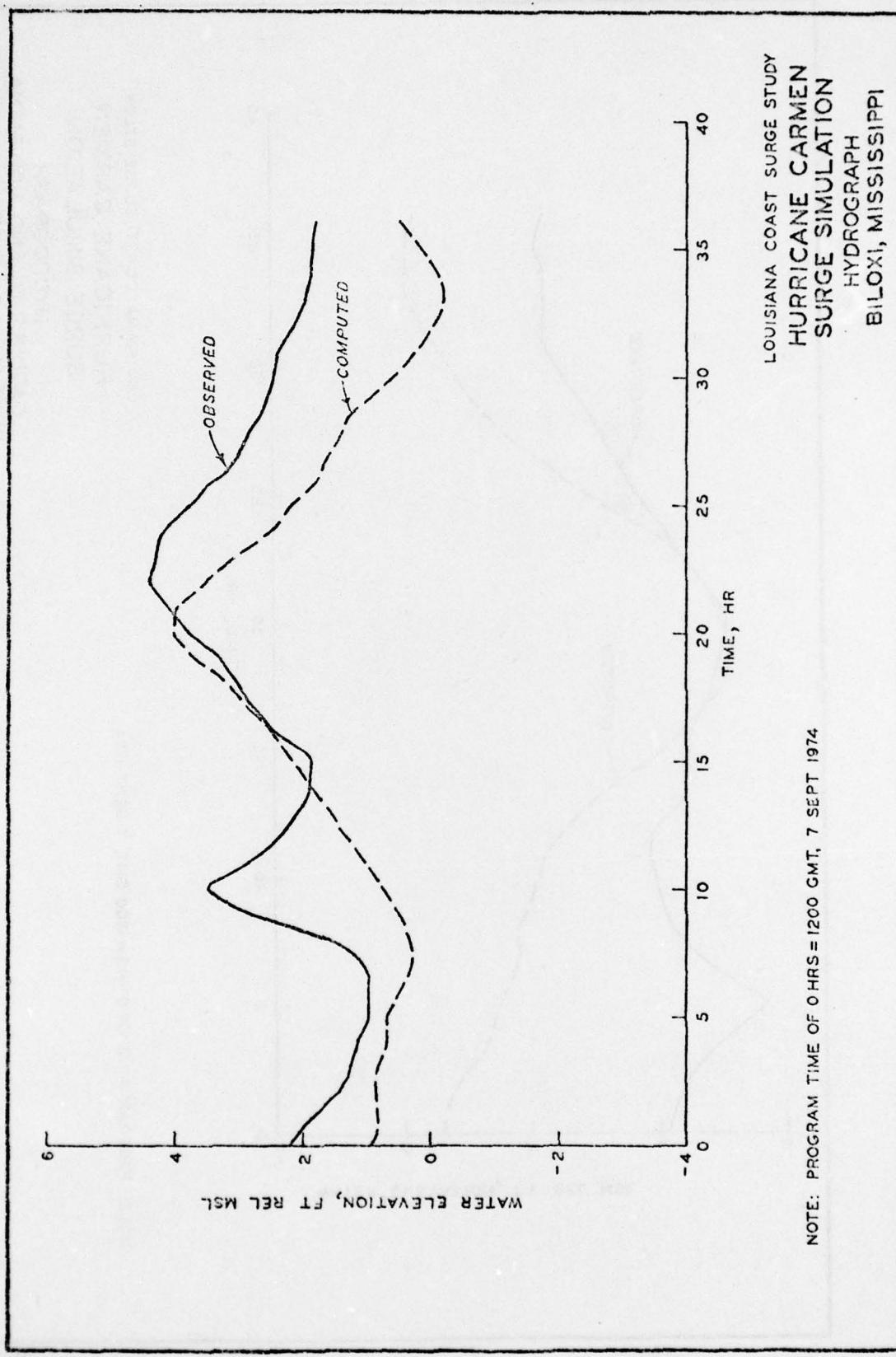
PLATE 39

APPENDIX A: NOTATION

A_b Storage area of the attached bay known as a function, H_b

A_c Channel cross-sectional area at mean sea level

A_I Surface area at mean sea level of the grid cell representative of H^+

A_s Surface area of the attached bay at mean sea level

B_n Transformation coefficients

C_d Nondimensional variable wind drag coefficient

C_n Transformation coefficient

C_D Nondimensional channel discharge coefficient

C_E Nondimensional coefficient for an overtopping barrier which is exposed on one side

C_S Nondimensional coefficient for a submerged barrier

D Depth of water $(H - D_o)$

D_o Local water depth relative to mean sea level

f Coriolis parameter

F Scale factor associated with the orthogonal curvilinear coordinate system

g Acceleration due to gravity

H Water level relative to mean sea level

H_b Water level relative to mean sea level in the ponding area

H_B Hydrostatic elevation of the sea surface corresponding to the departure of the atmospheric pressure from ambient

H^+ Predicted water level at the coast barrier without correction for flooding

IM,JM Number of grid points per computational lattice along the S and T axes

K_o Nondimensional variable seabed drag coefficient that depends on the seabed condition and water depth

L_c^k Length of coastline at unit elevations, Z_b^k, $k = 0,1,2...$

M_f Map factor relating prototype length to x,y units

P Atmospheric pressure

P_o Central atmospheric pressure of hurricane

P_∞ Far-field atmospheric pressure

A1

Q_S, Q_T	Volume transport per unit width in the S and T directions or, equivalently, in the local direction of ξ and η in prototype space
r_H	Distance from hurricane center to H grid points
R_H	Distance from the storm center to the region of maximum winds
S	Ordinate axis of the stretched shelf coordinate system
S_n, S_p	Distance normal to the seaward boundary and along the coast
T	Abscissa axis of the stretch shelf coordinate system
T_n	Long-wave travel time
T_x, T_y	The x and y components of the forward speed of this hurricane center
W_c	Bay entrance channel width
W_x, W_y	The x and y wind-speed components for a moving hurricane
W_R	The maximum wind speed for the stationary hurricane
W_{10}	Wind speed at an elevation 10 meters above the water surface
x	Rectilinear coordinate in prototype space
X_e	The x coordinate of the hurricane center in prototype space
X_g	The x coordinate of the H grid points in prototype space
y	Rectilinear coordinate in prototype space
Y_e	The y coordinate of the hurricane center in prototype space
Y_g	The y coordinate of the H grid points in prototype space
Z_b^k	Unit elevations of coastal barrier as denoted by $k = 0,1,2...$
β	The extent of η ($\pm$) in the image space of (ξ, η)
ΔS	Constant spaced computing grid increment between dependent variables in the S direction
Δt	Algorithm time increment between computing lattices
ΔT	Constant spaced computing grid increment between dependent variable in the T direction
η	The offshore curvilinear coordinate in prototype space and the abscissa in the image space of (ξ, η)
θ	The local angle between the ξ and x axis in prototype space
λ	The positive horizontal extent of the region to be mapped in prototype space and constrained to equal the extent of ξ in the image space.
μ, ν	Functions transforming ξ and η to the stretched shelf coordinate system (S,T)

ξ The alongshore curvilinear coordinate in prototype space and the ordinate in the image space of (ξ, η)

ϕ Hurricane wind ingress angle

ρ_a, ρ_w Density of air and water

σ_S, σ_T Seabed resistance stress divided by ρ_w in the S and T directions

$\tau_S \tau_T$ Wind stress divided by ρ_w in the S and T directions

In accordance with letter from DAEN-RDC, DAEN-ASI dated
22 July 1977, Subject: Facsimile Catalog Cards for
Laboratory Technical Publications, a facsimile catalog
card in Library of Congress MARC format is reproduced
below.